

**EFFECT OF PIPE INCLINATION ANGLE ON GAS-LIQUID FLOW USING  
ELECTRICAL CAPACITANCE TOMOGRAPHY (ECT) DATA**

A Thesis Presented to the Department of  
Petroleum Engineering

The African University of Science and Technology

In Partial Fulfilment of the Requirements  
For the Degree of

MASTER OF SCIENCE

By  
OTENG BISMARK

Abuja, Nigeria  
December, 2014

**EFFECT OF PIPE INCLINATION ANGLE ON GAS-LIQUID FLOW USING  
ELECTRICAL CAPACITANCE TOMOGRAPHY (ECT) DATA**

By

OTENG BISMARK

RECOMMENDED:

.....

Supervisor, Dr. Mukhtar Abdulkadir

.....

Professor Wumi Iledare

.....

Dr. Alpheus Igbokoyi

APPROVED:

.....

Head, Department of Petroleum Engineering

.....

Chief Academic Officer

.....

DATE

© Copyright by BISMARCK OTENG [2014]

All Rights Reserved

## ABSTRACT

Pipes that make up oil and gas wells are not vertical but could be inclined at any angle between vertical and the horizontal which is a significant technology of modern drilling. Experimental data on time varying liquid holdup for  $0^\circ$  and  $30^\circ$  pipe inclination angles were analyzed and interpreted. Parameters such as void fraction, slug frequency, lengths of liquid slug, Taylor bubble and slug unit, structure velocity and pressure drop were calculated from the experimental data. It was observed that an increase in pipe inclination from  $0^\circ$  to  $30^\circ$  brings about a corresponding reduction in average void fraction. Moreover, there is no particular correlation that gave better results in the two inclination angles based on the drift-flux model considered. The results of the comparison between the pressure gradient concerned with the  $0^\circ$  and  $30^\circ$  pipe inclination angles considered in this study using the Beggs and Brill (1973) correlation showed that the total pressure gradient increases with an increase in pipe inclination as a consequence of an increase in both gravitational and frictional pressure gradient. This study has provided useful information of the effect of pipe inclination on void fraction distribution using electrical capacitance tomography (ECT) data.

## **ACKNOWLEDGEMENT**

To my God who has been my glory and lifter-up of my head, I cannot thank you enough on this page, unto you be all the glory and honor forever more for bringing me this far. I could not simply have made it without you. My sincere gratitude goes to my supervisor Dr. Mukhtar Abdulkadir whose relentless effort has made this work a success, thank you sir for making it be. My next appreciation goes to my committee members Professor Wumi Iledera and Dr. Alpheus Igbokoyi; I appreciate your supports so much. To my parents and siblings especially my senior brother, Emmanuel Oteng, whose resources have made me come this far, may God reward you bountifully. I would not forget all the numerous friends and loved ones whose encouragements and supports saw me through my stay in AUST especially Deborah Boadu, when it looked impossible, you reminded me of the God under whose care there is nothing impossible; God richly bless you. Then to the Petroleum Engineering class of 2013/14, I say your support has been great. My gratitude goes to the multiphase flow in pipe group members for their unfailing support.

## **DEDICATION**

I dedicate this work to my parents and siblings, whose love, support and encouragement I can never forget.

# Contents

December, 2014 .....	i
ABSTRACT.....	iv
ACKNOWLEDGEMENT .....	v
DEDICATION.....	vi
LIST OF FIGURES .....	x
LIST OF TABLES.....	xii
Chapter 1.....	1
1.1    Introduction.....	1
1.3    Problem statement.....	4
1.4    Aim and Objectives.....	5
1.5    Structure of the thesis.....	5
Chapter 2.....	7
LITERATURE REVIEW .....	7
2.1    Gas-liquid flow in inclined pipes .....	7
2.2    Flow regime classification .....	12
2.2.1    Vertical flow regimes.....	13
2.2.1.1    Bubble flow pattern.....	14
2.2.1.2    Slug flow pattern.....	14
2.2.1.3    Churn flow pattern .....	15
2.2.1.4    Annular flow pattern .....	15
2.2.2    Horizontal flow regimes.....	16
2.2.2.1    Bubbly flow- .....	16
2.2.2.2    Stratified flow- .....	16
2.2.2.3    Stratified-wavy flow- .....	17
2.2.2.4    Plug flow-.....	17
2.2.2.5    Slug flow-.....	17
2.2.2.6    Annular flow-.....	17
2.2.2.7    Mist flow-.....	18
2.2.3    Flow pattern maps.....	18
2.2.3.1    Baker flow pattern map.....	19
2.2.4    Flow pattern identification .....	20

2.3	Tomographic techniques .....	25
2.4	Void fraction .....	26
2.4.1	Concept of void fraction .....	27
2.4.2	Classification of void fraction.....	28
2.4.3	The measurement principle .....	30
2.5	Void fraction correlations for inclined pipes .....	31
2.6	Drift flux correlations.....	32
2.7	Pressure drop in two-phase inclined pipes .....	33
Chapter 3.....		35
DATA ACQUISITION SETUP.....		35
3.1	Overview of the experimental facility.....	35
3.2	System (test fluid) .....	37
3.3	Parameters determined for this present study .....	38
3.3.1	Translational or rise velocity of Taylor bubble (structure velocity) .....	38
3.3.2	Determination of the distance ( $\Delta L$ ) between the two ECT planes.....	39
3.3.3	Determination of time delay .....	39
3.3.4	Slug frequency .....	40
3.3.5	Lengths of the slug unit, the Taylor bubble and the liquid slug.....	41
3.4	Summary .....	42
CHAPTER 4 .....		43
RESULTS AND DISCUSSION .....		43
4.1	Analysis of length; liquid slug, Taylor bubble and slug unit .....	43
4.2	Time and space average analysis .....	47
4.2.1	Mean void fraction from empirical correlations .....	50
4.3	Void fraction analysis .....	53
4.4	Pressure drop.....	57
4.5	Structure velocity .....	60
4.6	Flow pattern map .....	62
4.7	Probability density function (PDF).....	64
4.8	Frequency.....	67
CHAPTER 5 .....		70
CONCLUSIONS AND RECOMMENDATIONS .....		70



5.1	Conclusions.....	70
5.2	Recommendations.....	71
	NOMENCLATURE .....	72
	APPENDICES .....	74
	APPENDIX A DATA TEST MATRIX FOR 67mm 0o PIPE INCLINATION .....	74
	APPENDIX B DATA TEST MATRIX FOR 67mm 30° PIPE INCLINATION .....	77
	APPENDIX C BEGGS AND BRILL (1973) CORRELATION FOR PRESSURE GRADIENT .....	81
	CORRELATION PREDICTION FOR 67mm 0° PIPE INCLINATION.....	81
	APPENDIX D BEGGS AND BRILL (1973) CORRELATION FOR PRESSURE GRADIENT .....	83
	CORRELATION PREDICTION FOR 67mm 30o PIPE INCLINATION.....	83
	REFERENCES .....	86

## LIST OF FIGURES

Figure 2.1	-Upward vertical flow pattern- Taitel et al. (1980).....	14
Figure 2.2	Vertical flow patterns Abbas (2010).....	16
Figure 2.3	Flow- patterns- in- horizontal- gas-liquid -flows- Taitel (2000).....	18
Figure 2.4	Baker (1954) flow pattern map for horizontal flow in a tube. ....	20
Figure 2.5	a, b, c Flow identification by power spectrum density of pressure gradient Hubbard and Dukler (1966). Adapted from Hewitt (1978).....	21
Figure 2.6	Flow pattern identification by probability distribution function of void fraction Jones and Zuber (1975).....	22
Figure 2.6	(a) a single peak at low void fraction is indicative of discrete bubble flow.....	23
Figure 2.6	(b) a single peak at low void fraction accompanied by a long tail is indicative spherical cap bubble.....	23
Figure 2.6	(c) a double peak feature with the higher peak at low void fraction and the lower peak at a higher void fraction signifies stable slug flow.....	24
Figure 2.6	(d) a double peak feature with the lower peak at low void fraction and the higher peak at a higher void fraction signifies unstable slug flow.....	24
Figure 2.6	(e) a single peak at a high void fraction with a broadening tail is indicative of churn flow.....	25
Figure 2.6	(f) a single high peak at high void fraction is defined as annular flow.....	25
Figure 3. 1	The components of the rig (a) liquid pump (b) liquid tank (c) air-silicone oil mixing section (d) rotameters and (e) cyclone separator Abdulkadir (2011).....	36
Figure 3.2	Experimental flow facility Abdulkadir (2011b).....	37
Figure 3.3	Void fraction time series from the two ECT probes.....	40
Figure 4.1	a plot of length of liquid slug against gas superficial velocity for various liquid superficial velocities.....	44
Figure 4.2	a plot of length of slug unit against gas superficial velocity for various liquid superficial velocities.....	45
Figure 4.3	a plot of length of Taylor bubble against gas superficial velocity for various liquid superficial velocities.....	46
Figure 4.4	Effect of gas superficial velocity and angle of inclination on average void fraction at different liquid superficial velocity.....	49

Figure 4.5	(a) Experimental void fraction against empirical models for the <b>0°</b> inclination.....	50
Figure 4. 5	(b) Experimental void fraction against empirical models for the <b>30°</b> inclination .....	51
Figure 4.6	RMS of empirical correlation .....	52
Figure 4.7	a plot of void fractions in the Taylor bubbles against gas superficial velocity for various liquid superficial velocities .....	55
Figure 4.8	a plot of void fractions in the liquid slug against gas superficial velocity for various liquid superficial velocities .....	56
Figure 4.9	Influence of gas superficial velocity on gravitational and frictional pressure gradient .....	58
Figure 4.10	Influence of gas superficial velocities on the accelerational and total pressure gradient...	59
Figure 4. 11	Structure velocity for 0° and 30° inclination angles obtained from experiments using ECT and empirical correlations of Bendiksen (1984) and Nicklin et al. (1962) correlation.....	61
Figure 4.12	(a) and (b)Shoham (2006) flow pattern map for <b>0°</b> and <b>30°</b> air/silicone mixture .....	63
Figure 4.13	PDF for 0° and 30° pipe inclination .....	66
Figure 4.14	Effect of gas superficial velocity and angle of inclination on frequency for various liquid superficial velocity.....	66

## LIST OF TABLES

Table 3.1	Physical properties of air/silicon.....	38
Table 4.1	Average root mean square (ARMS) of empirical correlation for the 0° and 30° pipe inclination angles.....	51

# Chapter 1

## 1.1 Introduction

The simultaneous flow of several phases which may be a gas, liquid or a solid both in pipes and porous medium is referred to as multiphase flow. Brennen - (2005) defined multiphase flow as any fluid flow consisting of more than one phase or component. Multiphase flow has received both academic and industrial interest over the years because of its importance in nature and engineering applications.

Liquids transported in containers are subjected to splattering and unpredictable transient loads, which may affect the integrity of thin-shell containers, or make the transporting vehicle unstable Aydelott and Devol (1987). Typical practical situations where two-phase gas-liquid flow exists are in the nuclear, power, chemical and petroleum industries Brennen- (2005). For example, the calculation of pressure drop is reliant on the two - phase flow dynamics.

Multiphase flow in pipelines is a common occurrence in the petroleum industry Abdvayt (2003). According to Abdvayt (2003), multiphase flow in pipes which is known to be a common occurrence in the petroleum industry is usually conveyed through a single pipeline to storage facility since it is very expensive to separate the produced mixture of oil before transporting it. Multiphase flow exhibit several flow regimes in conduit depending on the gas and liquid flow rates and pipe inclination angle. Different inclinations will cause changes in the flow regime transitions and flow characteristics Kang et al. (1996). Measurement and prediction of liquid-gas multiphase flow regimes that occur in processing pipelines and wellbores are crucial to the petroleum industry. The understanding of the flow regimes is vital for engineers to

improve the configuration of pipelines and downstream processes to attain economic and safe design. Hence the ability to predict the multiphase fluid flow behavior of these processes is central to the efficiency and effectiveness of those processes Beggs (1973).

In the oil production systems, one component which has received much attention is the effect of pipe inclination on fluid flow, however there has not been enough experimental investigation using industry related fluids under various process conditions. The prediction of two-phase flow regimes in greater details with precision requires instrumentation that can measure and describe the flow within the pipes coupled with the use of more related industrial fluids. . This study seeks to investigate the effect of changing pipe inclination angle from  $0^{\circ}$  to  $30^{\circ}$  on gas-liquid flow using electrical capacitance tomography (ECT) data. The interest of this work is towards oil and gas industry applications.

## **1.2 Gas-liquid flow in inclined pipes**

The multiphase mixture is transported through a single pipeline to a central gathering station. It is very expensive to separate the produced mixture of oil and gas. During this transport, several flow regimes occur depending on the gas and liquid flow rates. The distances the multiphase mixture must be transported are often long and the deviations from horizontal flow are always present. These changes in inclination cause changes in the flow regime transitions and flow characteristics, which have a definite effect on the corrosion rate experienced by these pipelines Kang and Jepson (2002). In offshore operations very long pipelines are used to reach separation facilities sited at nearby platform or onshore. Separators, piping components or slug-catchers are used to control flow and processing during production and transportation of oil and gas, Shoham (2006). The application of

multiphase flows in the transportation of oil and gas through flow lines may be cost-effective for reservoir development. But, the hurdle to overcome is how to develop multiphase technology to transport oil and gas from subsea production units to processing facilities at nearby platforms or onshore separating facilities Zoetewij (2007).

The transportation of gas and liquid in conduits can lead to several topological configurations called flow patterns or flow regimes. This flow regime is usually observed when gas and liquid flow rates are sufficiently high. The simultaneous presence of gas and liquid in a pipe requires a more complex method of analysis than that applied to single phase flow problems. The composition variation of fluids inside this subsea flow line network can cause operational problems, such as non-continuous production or shut-down to damage equipment Beggs (1973).

Simultaneous production of gas-water and or oil-water mixtures may result in multiphase flow conditions in the flow line systems which connect the source to the production platform. As the production of the field progresses, the water content of the produced multiphase mixture increases to cause different mixture compositions, which affect the flow pattern and flow behavior Hernandez-Perez (2008).

As oil and gas reserves are being depleted in developed areas, activity is shifting to harsher and less accessible environments. This requires simultaneous transport of produced fluids to a land-based separation facility, with only minimal treatment offshore for such undesirable effects as corrosion, wax and hydrates Zheng et al. (1992).

Both the onshore and offshore cases can result in the simultaneous transport of oil and gas over long distances which require pipes which may be deviated from the horizontal Zheng et al., (1992). The accurate prediction of multiphase flow characteristics in these flow lines is required for the design, as well as the economical and safe operation of these transportation systems. Flow patterns are also dependent on the elevation profile of the pipeline Scott et al., (1990). For instance, flow patterns encountered in steeply inclined pipelines are different from those found in horizontal and near horizontal pipelines. The proper design of multiphase pipelines, together with downstream processing facilities, requires a thorough understanding of the behavior of multiphase flow in pipelines. As part of the scope of this study, this work seeks to evaluate the effects of pipe inclination and characterizing slug in pipes.

### **1.3 Problem statement**

Pipes that make up oil and gas wells are not vertical but could be inclined at any angle between the horizontal and the vertical which is a significant technology of modern drilling Zheng et al., (1992). Although extensive research in two-phase flow has been conducted during the last decades but most of this research has concentrated on either horizontal or vertical flow. Several good correlations exist for predicting pressure drop and liquid holdup in either horizontal or vertical flow, but these correlations have not been successful when applied to inclined flow.

Moreover many gathering lines and long-distance pipelines in the petroleum industry pass-through areas of hilly terrain therefore, in order to predict pressure drop, the liquid holdup must be accurately predicted Singh et al. (1970).



The ability to predict liquid holdup also is essential for designing field processing equipment, such as gas liquid separators. Hence, in order to accomplish a reliable design of gas-liquid systems such as pipe lines, boilers and condensers, a prior knowledge of the flow pattern is needed.

#### **1.4 Aim and Objectives**

The aim of this research is to investigate the effect of pipe inclination on void fraction distribution. In order to achieve the aim the following objectives will be met

- 1.) To analyze raw experimental ECT data obtained from an experimental investigation carried out by Abdulkadir, (2011) using air-silicone oil mixture in a 67 mm diameter pipe inclined at  $0^\circ$  and  $30^\circ$  from the horizontal.
- 2.) To characterize the hydrodynamics of slug flow both in the  $0^\circ$  and  $30^\circ$  pipe inclination via the determination of the following: the translational velocity, void fraction in the liquid slug, void fraction in Taylor bubble, length of liquid slug and Taylor bubble, the frequency of slugging and the pressure drop.

#### **1.5 Structure of the thesis**

The layout of this thesis is summarized as follows;

Chapter 1-Introduction- This Chapter provides an introduction to the thesis, defining the problem, aim and objectives of the study, methodology and the structure of the thesis.

Chapter 2-Literature Review - This chapter is concerned with review of published work on void fraction distribution in pipes. Flow pattern transition, maps and identification in vertical, horizontal and inclined pipes for two-phase flow was reviewed followed by void fraction

concept and correlations for inclined pipes. A pressure drop correlation for upward inclined two-phase flows was also reviewed.

Chapter 3-Data Acquisition Setup - This chapter describes the experimental facility that was used to measure the time varying liquid holdup for this work.

Chapter 4-Results and Discussion- This chapter looks at the results obtained from the experimental flow facility and critical analysis of the results to achieve the objectives stated.

Chapter 5 - Conclusions and recommendations - This chapter brings together all the key conclusions from this work and provides some recommendations.

## Chapter 2

### LITERATURE REVIEW

Two-phase gas-liquid flow is a common phenomenon in nuclear reactors, chemical reactors, power generation, process industries and petroleum industries Abduvayt (2003). In multi-phase flow studies, gas-liquid flows are the most studied compared to other types of flow. The behavior of two-phase gas-liquid flow compared to a single phase flow of either a gas or liquid is significantly different. In order to predict and control two-phase flow behavior and its corresponding pressure drop, heat transfer and mass transfer characteristics, a good understanding of the hydrodynamics of the system is required. This chapter deals with the fundamentals of two-phase gas-liquid flows with emphasis on pipe inclination. It will also discuss flow pattern maps and the methods of their identification

#### 2.1 Gas-liquid flow in inclined pipes

The study of two-phase gas- liquid flow in inclined pipes for the last few decades are summarized below, it outlines the experiment conducted and the parameters involved. Two-phase gas-liquid flow was investigated in theoretical and experimental studies. Most data reported on flow pattern transitions have dealt with either horizontal or vertical tubes with only limited results reported for inclined pipes.

Sevigny (1962) conducted a comprehensive study of two-phase flow in inclined pipes. Air and water were the test fluids in 20 mm ID pipe with varying pipe inclinations. He found that pressure gradients are greatly affected by inclination angles.

Zukoski (1966) studied the effect of pipe inclination angle on bubble rise velocity in a stagnant liquid. He concluded that, depending on the pipe diameter, surface tension and viscosity of fluids

may appreciably affect the bubble rise velocity. His findings also showed that for some conditions an inclination angle as small as  $1^\circ$  from the horizontal can cause the bubble rise velocity to be more than 1.5 times the value obtained for horizontal pipes.

A study of slug flow in inclined pipes was reported by Singh and Griffith (1970). They measured pressure drop and liquid holdup in pipe with diameters of 0.626, 0.822, 1.063, 1.368, and 1.600 in. (16-40 -mm), at inclination angles of plus and minus  $10^\circ$  and  $5^\circ$  from horizontal, and at  $0^\circ$ . Liquid holdup was found to be independent of inclination angle.

Bonnecaze et al. (1971) developed a model for two phase flow in inclined pipeline and claimed that pressure drop was a strong function of the liquid holdup in the slug unit.

Later, Beggs (1972) used a 50.8 and 62.9 mm ID pipe and carried out a study of inclination effects. He experimentally showed that liquid holdup was strongly affected by pipe inclination angle.

Mattar and Gregory (1974) conducted experiments to find the effect of inclination on slug velocity, holdup and pressure gradient. They found that for uphill pipe sections, slug flow was the predominant flow pattern, and for downhill pipe sections stratified flow dominated. They also observed that hydrostatic head for slug flow dictated pressure gradient in uphill sections.

Gould et al. (1974) published flow pattern maps for horizontal and vertical flow and for up-flow at  $45^\circ$  inclinations.

Later, Spedding and Chen (1981) experimentally studied pressure drop in two phase flow in inclined pipe corroborating the relationship between flow pattern and pressure drop.

In 1985, Barnea et al examined the effect of the inclination angle on the flow pattern transition boundaries by varying the inclination angle in small steps in the range of  $0^\circ$  to  $90^\circ$ . They found that small changes in the angle of inclination from the horizontal can have profound effects on

the flow patterns that exist. At very small inclination angles, the force of gravity acting in the flow direction can be of the order of the wall shear stress. On the other hand, small deviations from the vertical have little effect on flow patterns.

Kokal and Stanislav (1989) showed that the uphill-flow regimes were found to be similar to the horizontal-flow regimes except that very limited stratified flow was observed for uphill flows. The downhill-flow regimes on the other hand were found to be very different and more complex.

Xiao et al. (1990) developed a comprehensive mechanistic model for gas-liquid two-phase flow in horizontal and near-horizontal pipelines. The comprehensive mechanistic model incorporated flow pattern prediction capabilities. Separate models could then be used to calculate different flow characteristics like liquid holdup and pressure gradients. The model was validated with a comprehensive databank.

Roumzeilles et al. (1994) performed an experiment on downward simultaneous flow of gas and liquid in hilly terrain pipelines and injection wells. They developed most of the methods for predicting pressure drop in gas-liquid two phase flow in pipes for either upward vertical or upward inclined pipe. They investigated experimentally downward concurrent slug flow in inclined pipe via obtaining liquid holdup and pressure drop measurements for downward inclination angles from  $0^\circ$  to  $30^\circ$  at different flow condition.

Cook and Behnia (2000) presented a comprehensive treatment of all sources of pressure drop within intermittent gas-liquid flows. Calculated pressure loss associate with the viscous dissipation within a slug, and the presence of dispersed bubbles in a slug were accounted for, without recourse to the widely used assumption of homogenous flow. The results show that

existing intermittent flow models predict pressure gradients considerably lower than were observed.

Colmenares et al. (2001) studied pressure drop models for horizontal slug flow for viscous oils. Their experimental results suggested that the slug flow region in the flow pattern map was enlarged when the oil viscosity increased. Experimental results from a 0.48 Pas viscous liquid-gas two-phase flow also concluded that as liquid viscosity increased, slug frequency and liquid film holdup increased while the slug length decreased.

Lewis, et al. (2002) discussed utility of the hot-film anemometry technique in describing the internal flow structure of a horizontal slug flow pattern within the scope of intermittent nature of slug flow. It was shown that a single probe can be used for identifying the gas and liquid phases and for differentiating the large elongated bubble group from the small bubbles present in the liquid slug.

Zhang et al.(2003) developed a unified hydrodynamic model to predict flow pattern transitions, pressure gradient, liquid holdup and slug characteristics in gas-liquid pipe flows for all inclination angles (from  $-90^{\circ}$  to  $90^{\circ}$  from horizontal).

Gokcal (2005) experimentally studied the effects of high viscosity liquids on two-phase oil-gas flow. He observed a marked difference between the experimental results and the model predictions. Intermittent slug and elongated bubble flow were the dominant flow pattern.

Later, Ribeiro, et al. (2006) compared new data on pressure drop and liquid hold-up obtained in a horizontal square cross-section channel against several existing correlations and models for gas liquid flow. The hold-up data were taken for conditions of wavy stratified and pseudo-slug flow. Pressure drop results were only obtained for wavy stratified flow.

Wongwises and Pipathattakul (2006) studied experimentally two phase flow pattern, pressure drop and void fraction in horizontal and inclined upward air–water two-phase flow in a mini-gap annular channel. They observed and recorded the flow phenomena, which are plug flow, slug flow, annular flow, annular/slug flow, bubbly/plug flow, bubbly/slug–plug flow, churn flow, dispersed bubbly flow and slug/bubbly flow by high-speed camera. Also a slug flow pattern was found only in the horizontal channel while slug/bubbly flow patterns are only in inclined channels. When the inclination angle was increased the onset of transition from the plug flow region to the slug flow region (for the horizontal channel) and from the plug flow region to slug/bubbly flow region (for inclined channels) shift to a lower value of superficial air velocity.

Gokcal (2008) later conducted an experimental study to develop closure relationships for two-phase slug flow characteristics for high viscosity oils. The parameters that he considered include pressure gradient, drift velocity, translational velocity, slug length and slug frequency. All tests were conducted for horizontal flow and oil viscosities range from 0.181 Pas to 0.585 Pas.

Hernandez-Perez et al. (2010) studied the effect of pipe inclination on the internal structure of a liquid slug body at different pipe inclination angle from the horizontal to vertical. The working fluid employed in the experiment was air and water with a pipe diameter of 67 mm using WMS to take measurements. The superficial gas and liquid velocity are  $0.2ms^{-1}$  and  $0.7ms^{-1}$ , respectively. However, it was revealed in their work that void fraction distribution was strongly affected by pipe inclination, but does not strongly affect the bubble size distribution and they finally concluded that there exist a relationship between void fraction and bubble size distribution in a liquid slug body.

Arvoh et al.(2012) used a combination of gamma measurements and multivariate calibration to estimate multiphase flow mixture density and to identify flow regime. The experiments were

conducted using recombined hydrocarbon. These were conducted at a temperature of 0°C and a 75-bar pressure. Two angles of inclination (1° and 5°) and two water cuts (15% and 85%) were investigated. The estimated mixture densities were accurate as compared with those from the single-energy gamma densitometer with a root mean square error of prediction of 13.6 and  $9.7 \frac{kg}{m^3}$  for 1° angle of inclination and 17 and  $26.6 \frac{kg}{m^3}$  for 5° pipe inclination. Flow patterns observed in upward inclined flow are quite similar to those observed in vertical upward flow, especially for near-vertical systems. They include bubbly and dispersed bubbly, slug, churn and annular flow in inclined systems.

Esam and Riydh (2013) studied flow pattern and pressure drop of gas–liquid flow in inclined pipe experimentally. The diameter of test section is 50 mm, and overall length of 4 m. The inclination angle of the test section is 30°. Air and water are used as working fluids. The experimental results showed that the inclination angle has a significant effect on the flow pattern transition and pressure drop. It was noted that the pressure decreases with distance along pipe when gas superficial velocity increased and also increased liquid superficial velocity. And the slug liquid appears when the fluctuation in pressure accrues. The liquid holdup decreased when increased gas superficial velocity and depends on the flow pattern.

## **2.2 Flow regime classification**

The variation in physical distribution of fluid phases during multiphase flow through conduits or pipes is called flow regime (flow pattern). Numerous investigations have been carried out in identifying flow regimes and the transitions between them. Detailed reviews of earlier work which focuses on two phase flow patterns and pattern transition have been published by Govier and Aziz (1972), Hewitt (1982) and Delhaye et al. (1981). Recent experimental and semi theoretical studies reviews have been provided by Thomas and Collier (1994). In the



simultaneous flow of two-phases in pipes, the fluids tend to exhibit a number of different flow regimes. The flow regime exhibited is dependent on the relative magnitude of flow rate, pipe diameter, pipe inclination angle and fluid properties (density and viscosity). In wellbores several different flow regime can exist due to the large pressure and temperature changes encountered during upward flow of fluids Mukherjee et al. (1999). Knowledge of the flow pattern is vital to define fluid mechanics in multiphase flow and also for successful operation in oil production from older subsea oil wells. Usually flow regimes are grouped under horizontal, vertical, and inclined pipes orientation. According to Legius (1997), multiphase flow in vertical pipes, exhibits; bubbly, slug, churn or annular flow patterns and in horizontal and in - inclined pipes, these flow patterns are extended to include smooth stratified, stratified wavy and plug flows.

### 2.2.1 Vertical flow regimes

In two-phase gas-liquid flow in pipes or channels, an interface exists between the phases. The phase boundary can take a variety of configurations, known as the flow pattern. The existing flow pattern in a given two-phase flow system depends on the operational parameters (gas and liquid flow rates), the geometrical variables (pipe diameter and pipe inclination angle), and the physical properties of both phases (gas and liquid densities, viscosities and surface tension) Elekwachi (2008). According to Beggs and Brill (1994), they described the four flow observed in gas-liquid flow in vertical pipe as bubble flow, slug flow, transition (annular-slug transition) flow and mist (annular-mist) flow. For upward multiphase flow of gas and liquid, the most described by Taitel et al. (1980) are namely- bubble flows, slug flow, churn flow and annular flow. These flow patterns, shown in Figure 2.1, are described in order of increasing gas flow rate.

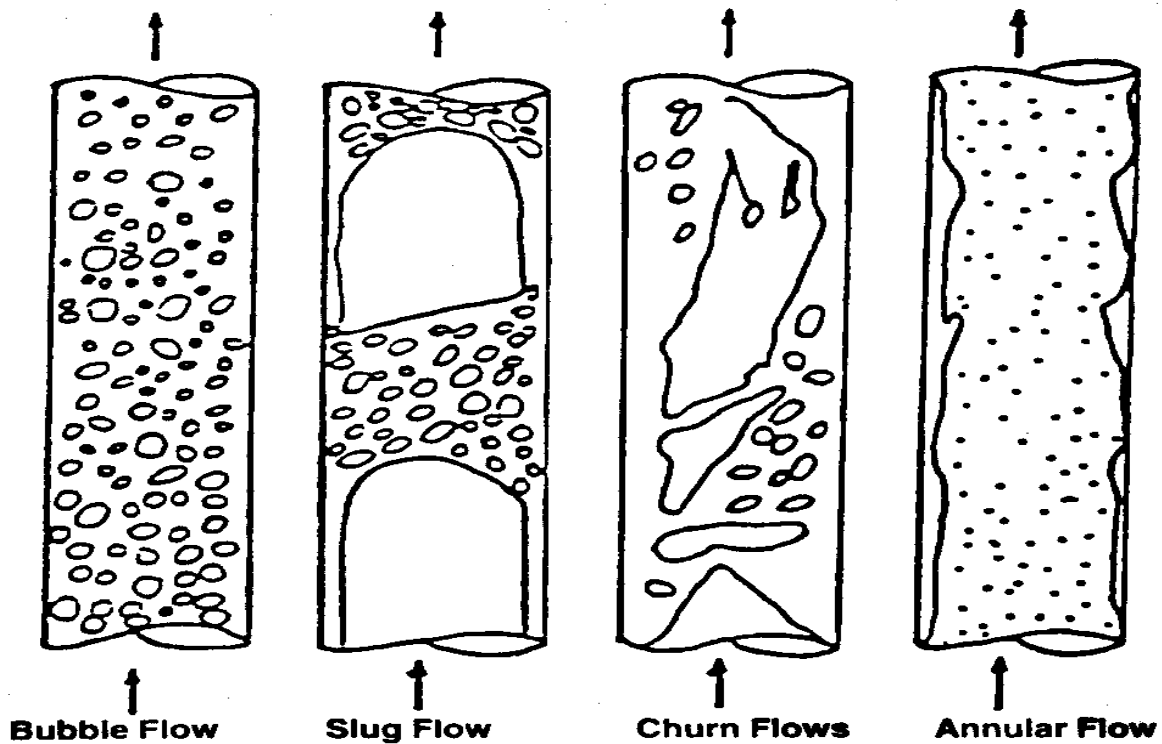


Figure 2.1 -Upward vertical flow pattern- Taitel et al. (1980)

2.2.1.1 Bubble flow pattern- In the bubble flow pattern, the liquid phase almost completely fills the pipe and the gas is present in the liquid as small bubbles and is randomly distributed. The diameters of the bubbles vary randomly. At high gas flow rate, the number of bubbles in solution increases resulting in frequent collisions between the bubbles. This causes more bubbles to coalesce. Griffith and Wallis (1961) noted that the bubble/slug transition occurs at a void fraction of about 0.25 - 0.30.

2.2.1.2 Slug flow pattern- The gas phase is more dominant in the slug flow although liquid phase is still continuous. The gas bubbles merge with each other to form stable bubbles of almost equal shape and size which are approximately the same diameter of the pipe. These

bubbles formed are called Taylor bubbles. Slug flow consists of successive Taylor bubbles and liquid slug which link the entire pipe cross section. In between the Taylor bubbles and the pipe wall there exist a thin liquid film, these film enters into the following liquid slug and produce a mixing zone aerated by small gas bubbles Taylor et al. (1950)-According to Jayanti and Hewitt (1992), four major theories have been proposed to explain the transition from slug flow to churn flow in vertical pipes. These mechanisms are entrance effect, flooding, wake effect and bubble coalescence mechanisms.

2.2.1.3 Churn flow pattern- Churn flow is chaotic flow of gas and liquid also referred to as froth flow and semi-annular flow is a highly disturbed flow of gas and liquid in which both the shape of the Taylor bubble and liquid slug are distorted by increase in the gas velocity which causes the liquid slug to become unstable, leading to its break-up and fall. This liquid merges with the approaching slug, which then resumes its upward motion until it becomes unstable and falls again. The alternating direction of motion in the liquid phase in irregular manner is typical of churn flow, Brill and Mukherjee (1999).

2.2.1.4 Annular flow pattern- Annular flow is also referred to as mist or annular-mist flow Duns and Ros (1963) and Aziz and Govier (1972). It is characterized by a central core of fast flowing gas and a slower moving liquid film that travels around the pipe wall. The shearing action of the gas at the gas-liquid interface generates small amplitude waves (ripples) on the liquid surface. By increasing the flow conditions beyond critical gas and liquid flow rates, large amplitude surges or disturbance waves occur.

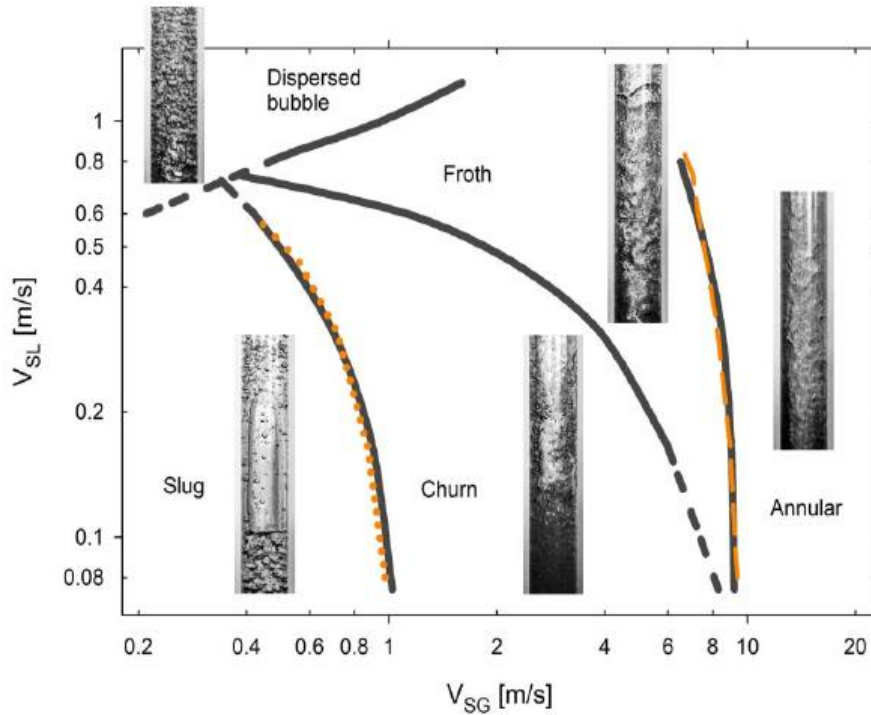


**Figure 2.2 Vertical flow patterns Abbas (2010)**

### 2.2.2 Horizontal flow regimes

Two phase flow patterns in horizontal tubes are similar to those in vertical flows but the distribution of the liquid is influenced by gravity that acts to ensure the liquid is confined at the bottom of the tube and the gas at the top. Flow patterns for co-current flow of gas and liquid in a horizontal pipe are characterized as follows Taitel (2000)

2.2.2.1 Bubbly flow- The gas bubbles are dispersed in the liquid with a high concentration of bubbles in the upper half of the pipe due to their buoyancy. When shear forces are dominant, the bubbles tend to disperse uniformly in the pipe. In horizontal flows, the regime typically only occurs at high mass flow rates Loilier (2006).

2.2.2.2 Stratified flow- At low liquid and gas velocities, complete separation of the two phases occurs. The gas goes to the top and the liquid to the bottom of the tube, separated by an

undisturbed horizontal interface. Hence, the liquid and gas are fully stratified in this regime Loilier (2006).

2.2.2.3 Stratified-wavy flow- Further increasing the gas velocity, these interfacial waves become large enough to wash the top of the tube. This regime is characterized by large amplitude waves intermittently washing the top of the tube with smaller amplitude waves in between. Large amplitude waves often contain entrained bubbles. The top wall is nearly continuously wetted by the large amplitude waves and the thin liquid films left behind Loilier (2006).

2.2.2.4 Plug flow- This flow regime has liquid plugs that are separated by elongated gas bubbles. The diameters of the elongated gas bubbles are smaller than the tube, such that, the liquid phase is continuous along the bottom of the tube below the elongated bubbles. Plug flow is also sometimes referred to as elongated bubble flow Taitel (2000).

2.2.2.5 Slug flow- At higher gas velocities, the diameters of elongated bubbles become similar in size to the channel height. The liquid slug separating such elongated bubbles can also be described as large amplitude waves Taitel (2000).

2.2.2.6 Annular flow- At even larger gas rates, the liquid forms a continuous annular film around the perimeter of the tube, similar to that in vertical flow but the liquid film is thicker at the bottom than the top. The interface between the liquid annulus and the vapor core is distributed by small amplitude waves and droplets may be dispersed in the gas core. At high gas fractions, the top of the tube with its thinner film becomes dry first, so that the annular film covers only part of the tube perimeter and thus this is then classified as stratified-wavy flow Taitel (2000).

2.2.2.7 Mist flow- Similar to vertical flow, at very high gas velocities, all the liquid may be stripped from the wall and entrained as small droplets in the continuous gas phase (Thome, 2007). Taitel (2000) represents the different co-current flow regimes of gas and liquid that can be encountered in a horizontal pipeline

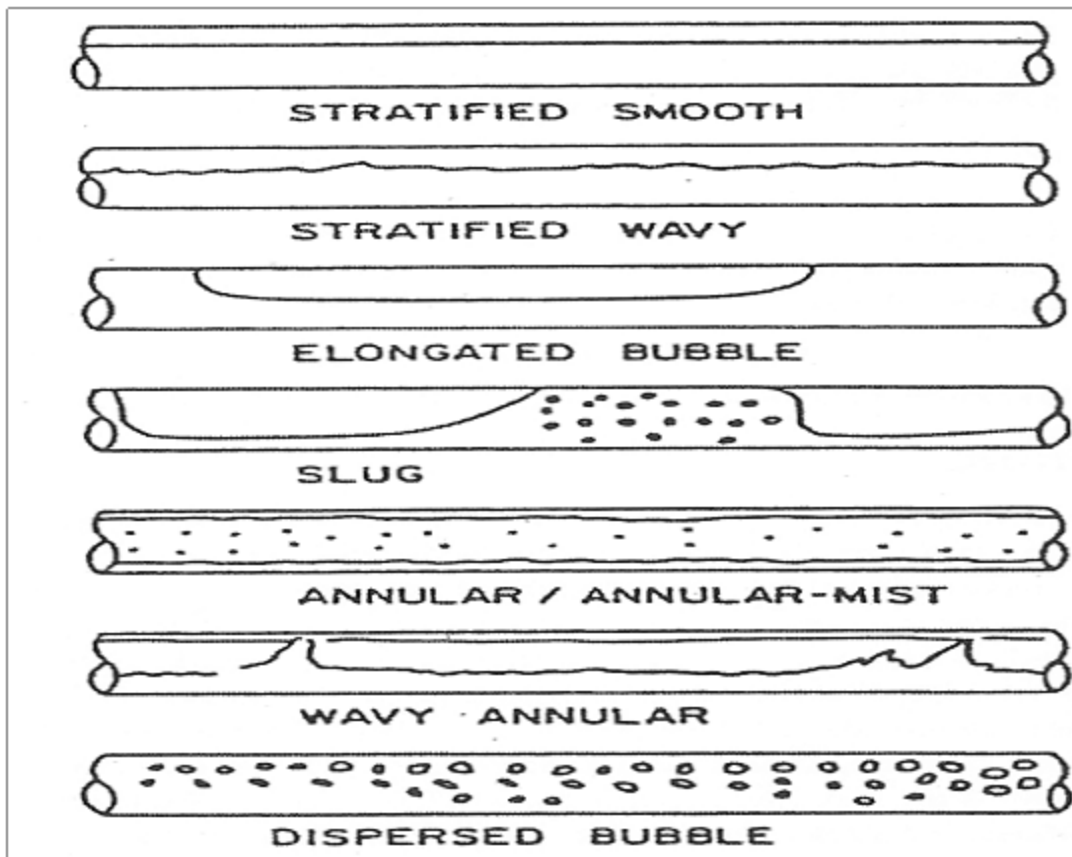


**Figure 2.3 Flow-patterns- in- horizontal- gas-liquid -flows- Taitel (2000)**

2.2.3 Flow pattern maps

A flow pattern map is a representation of the existence of flow patterns in a two dimensional domain in terms of system variables. They consist of flow regimes separated by transition lines and are gotten from the description and classification of the various flow patterns Omebere-Iyari (2006). The flow pattern that can be observed is dependent on- the fluid properties, flow rates,

pipe diameter, pipe inclination angle, and operating conditions at ends of the pipe. The accurate prediction of the flow pattern existing under a given conditions is required, since every flow pattern has a unique hydrodynamic characteristics.

### 2.2.3.1 Baker flow pattern map

The first to recognize the importance of the flow pattern as a starting point for the calculation of pressure drop, void fraction, and heat and mass transfer was Baker (1954). He published the earliest flow pattern map for horizontal flow, presented below. To utilize this map, first the mass velocities of the liquid  $G_L$ -and vapor  $G_G$  -must be determined. Then the gas-phase parameter  $\lambda$  and the liquid-phase parameter  $\psi$  are calculated as follows:

$$\lambda = \left( \frac{\rho_G}{\rho_{air}} \frac{\rho_L}{\rho_{water}} \right)^{1/2} \dots \dots \dots (2.1)$$

$$\psi = \left( \frac{\sigma_{water}}{\sigma} \right) \left[ \left( \frac{\mu_L}{\mu_{water}} \right) \left( \frac{\rho_{water}}{\rho_L} \right)^2 \right]^{1/3} \dots \dots \dots (2.2)$$

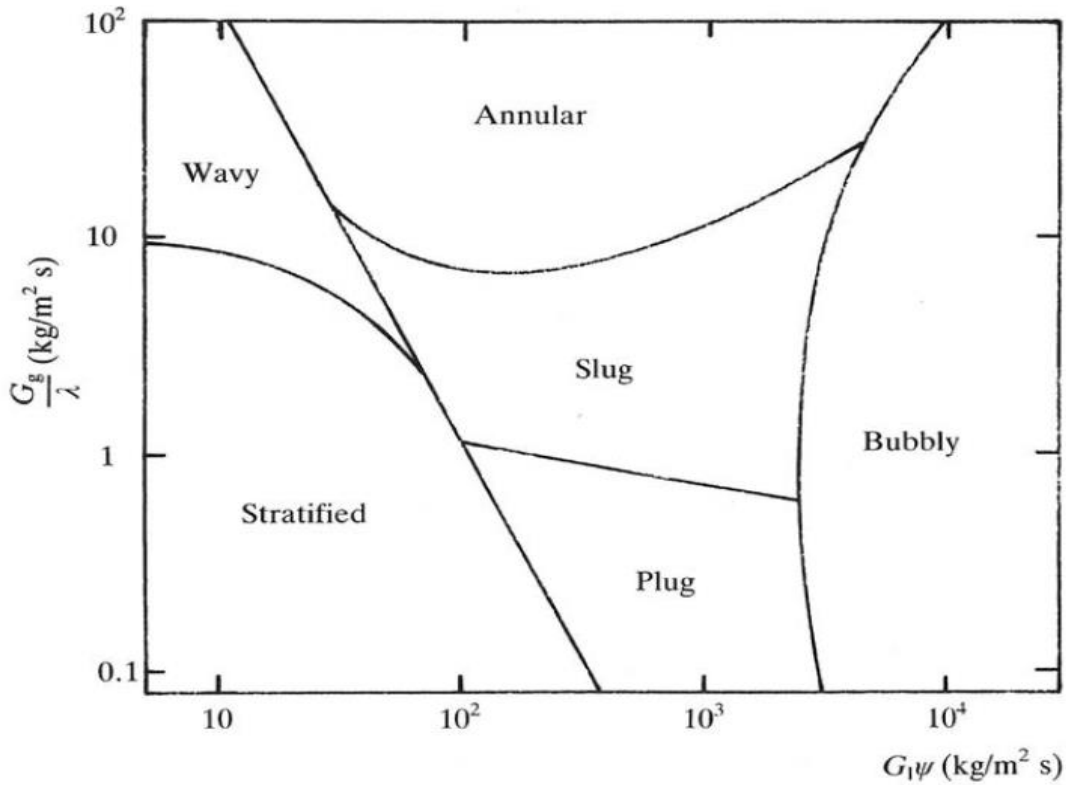


**Figure 2.4 Baker (1954) flow pattern map for horizontal flow in a tube**

Where  $\rho_G, \rho_L, \mu_L$  and  $\sigma$  are the properties of the fluid and  $\rho_{Water}, \rho_{air}, \mu_{Water}$  and  $\sigma_{Water}$  are the reference properties of air and water at standard atmospheric pressure and room temperature. The map shown in Figure 2.4 was developed based on air - water data.  $\lambda$  and  $\psi$  are standard dimensionless parameters that should take into account the variation in the properties of the fluid.

#### 2.2.4 Flow pattern identification

Gas-liquid flow pattern can be identified by observing visually the flow in transparent pipes. But this has its own limitations and cannot be done all the time because; high gas and liquid flow rates will make visual observation impossible. Hence high speed photography is often used. The above two methods are not applicable in the industries because, actual industrial pipes are not



transparent, Hernandez-Perez (2008). Hubbard and Dukler (1966) also developed a method for flow regime determination, which employs spectral analysis to study the observed pressure fluctuations. The technique is based on the idea that, the gas-liquid flow patterns are characterized by fluctuations in wall pressure. The power spectral density (PSD) of digitized time response, gotten from a pressure transducer located flush to the wall of the flow pipe was calculated from autocorrelation method. Three types of power spectral distributions were obtained and used to group the various flow regimes measured for horizontal air-water pipe flows. These are shown in Figure 2.5, namely- (a) separated flows; containing a peak at zero frequency; this type of response is obtained from stratified and wavy flows, (b) dispersed flows; possessing a flat and relatively uniform spectrum and (c) intermittent flows; with a characteristic peak; this is obtained for plug and slug flows.

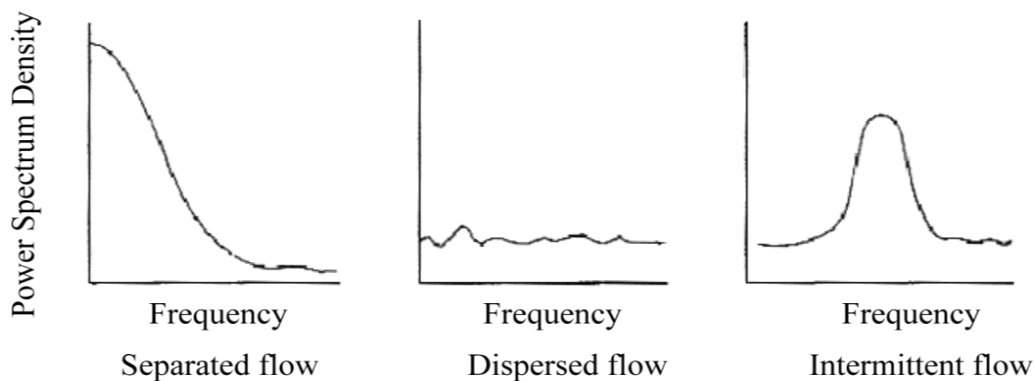


**Figure 2.5 a, b, c Flow identification by power spectrum density of pressure gradient Hubbard and Dukler (1966). Adapted from Hewitt (1978)**

This was the first effort to categorize flow patterns centered on proofs and was monitored by the studies carried out by Nishikawa et al. (1969) and Kutataledze (1972). Investigations by Tutu (1982) and Matsui (1984), analyzed the time variation of pressure gradient and pressure fluctuations, respectively. Tutu (1982) used the probability density distribution to identify the

flow patterns observed in vertical flow systems. But, Keska and Williams (1999) established that the pressure system Tutu investigated did not offer a better flow pattern recognition method relative to capacitive and resistive systems. Vince and Lahey (1982) obtained a series of chordal-averaged void fraction measurements using a dual beam x-ray system for low pressure air-water flow in a vertical pipe. Their results were used to generate corresponding PDF and PSD functions of the recorded signals. They observed that the calculated moments were responsive to the velocity of the liquid phase. Jones and Zuber (1975) advocated the use of the photon attenuation technique, to measure the time-varying, cross-sectional averaged void fraction. This system used a dual x-ray beam device for a two-phase mixture of air and water, flowing vertically. It was observed that the probability density function (PDF) of the void fraction fluctuations shown in Figure 2.6 could be used as an objective and measurable flow pattern discriminator.

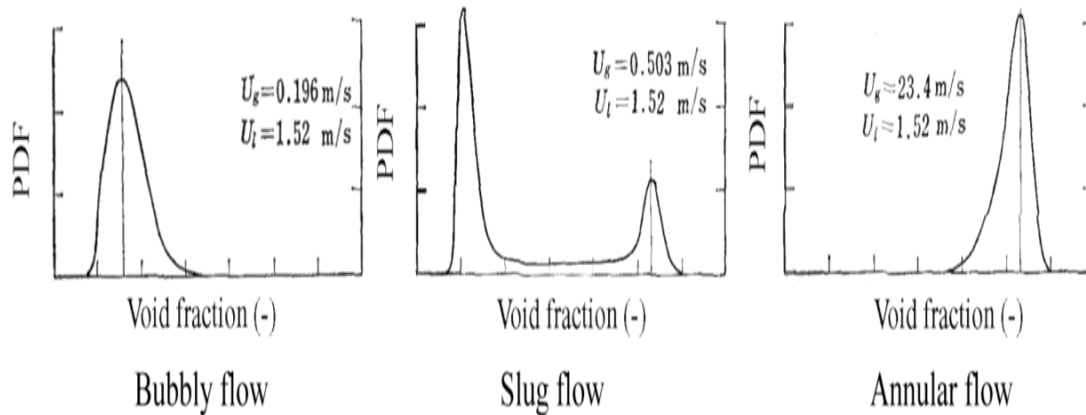


**Figure 2.6 Flow pattern identification by probability distribution function of void fraction Jones and Zuber (1975)**

Costigan and Whalley (1997) upgraded the PDF methodology of Jones and Zuber using segmented impedance electrodes and successfully grouped flow patterns into six: discrete bubble, spherical cap bubble, stable slug, unstable slug, churn and annular. Figure 2.6(a) to 2.6(f)

shows the Void fraction traces and corresponding PDFs of the six flow patterns respectively, from Costigan and Whalley (1997):

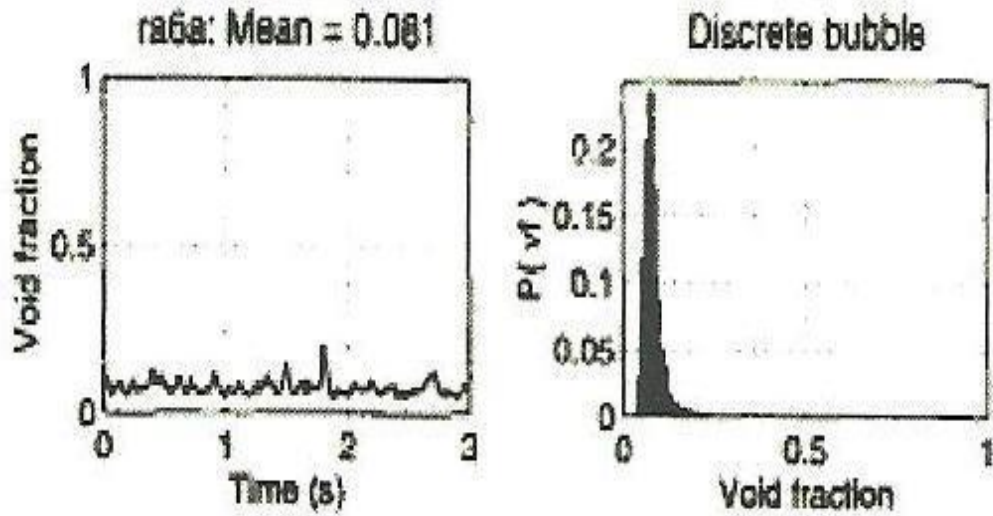


Figure 2.6 (a) a single peak at low void fraction is indicative of discrete bubble flow

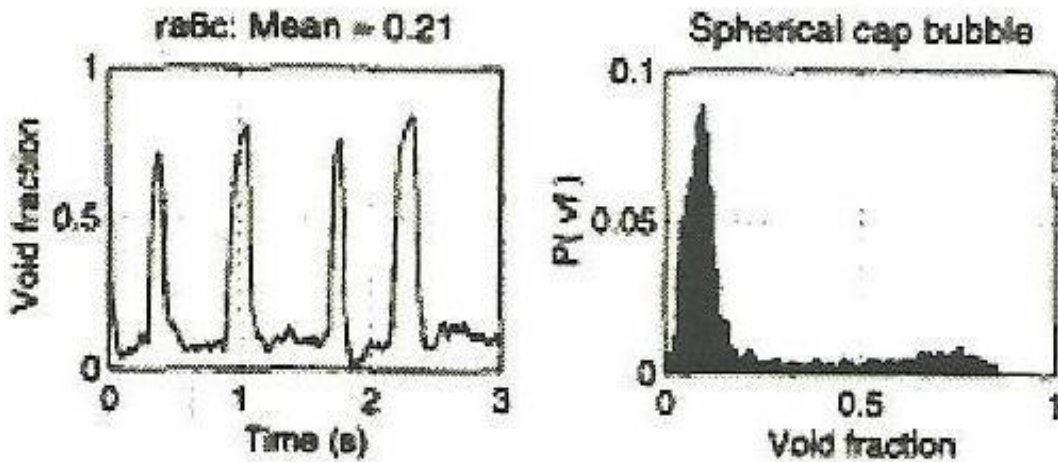


Figure 2.6 (b) a single peak at low void fraction accompanied by a long tail is indicative spherical cap bubble.

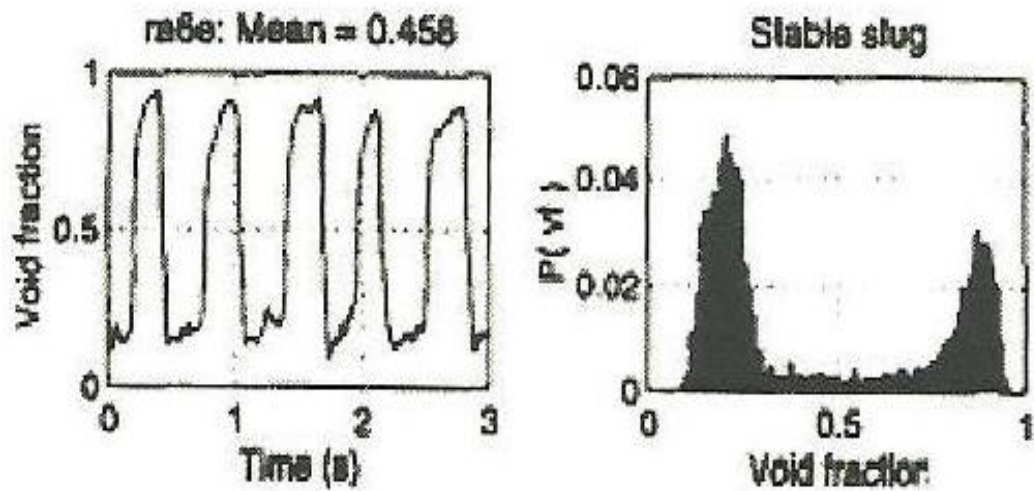


Figure 2.6 (c) a double peak feature with the higher peak at low void fraction and the lower peak at a higher void fraction signifies stable slug flow

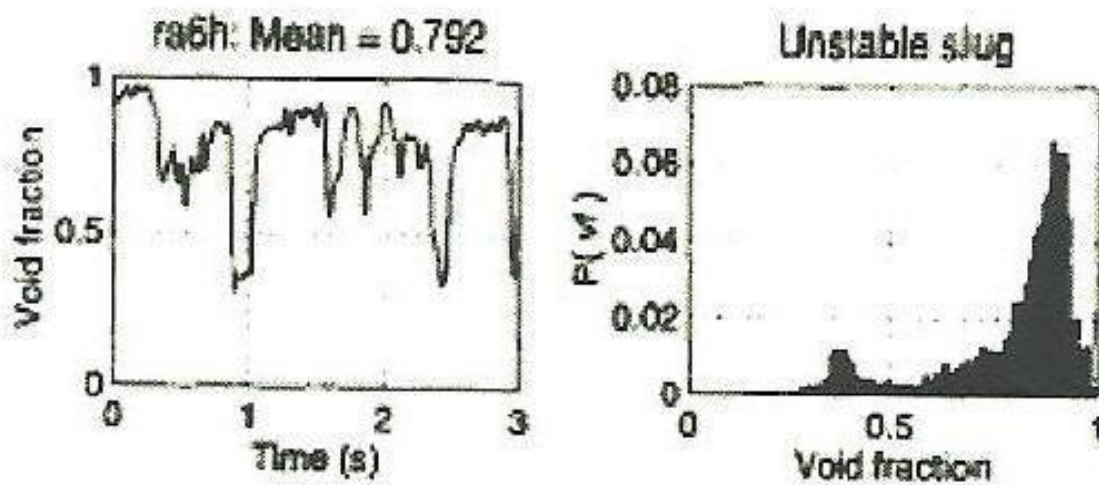


Figure 2.6 (d) a double peak feature with the lower peak at low void fraction and the higher peak at a higher void fraction signifies unstable slug flow

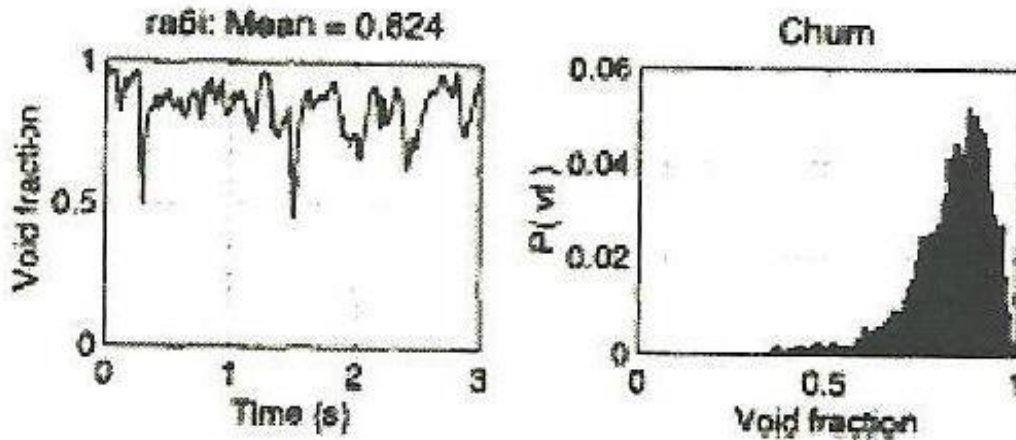


Figure 2.6 (e) a single peak at a high void fraction with a broadening tail is indicative of churn flow

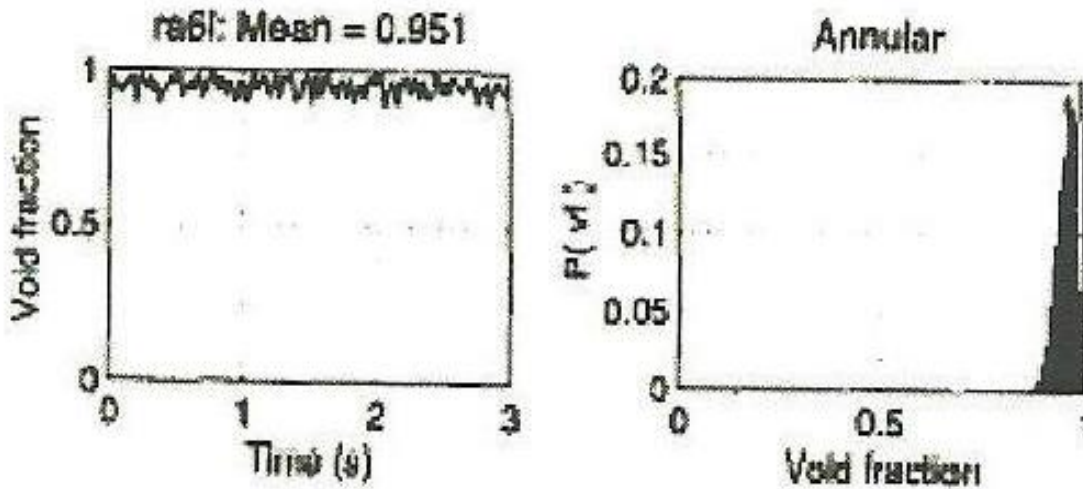


Figure 2.6 (f) a single high peak at high void fraction is defined as annular flow

### 2.3 Tomographic techniques

Tomography is a non-invasive imaging technique allowing for visualization of the internal structure by the use of any kind of penetrating wave. Alternatively, the term tomography usually refers to a technique that enables the determination of the density distributions in a cross-section of an object. A tomograph is a device used in tomography, while the image produced is a tomogram. The two types of tomographic techniques are intrusive and non-intrusive. Shemer et

al. (2006) describes the later method as it uses either a set of radiation attenuation measurements such as x-ray,  $\gamma$ -ray, sound waves or impedance measurements among various pairs of electrodes glued flush to the pipe surface. Kumar et al.(1995) used a computed tomographic scanner using  $\gamma$ -ray for measuring void fraction distribution in two phase flow system such as fluidized beds and bubble columns. Creutz and Mewes (1998) also employed an electro-resistance tomography to measure the concentration distribution inside a gas-liquid centrifugal pump. In addition, an x-ray tube and scintillating detectors were used by Kendoush and Sarkis (2002) for void fraction measurements.

In this thesis work, liquid hold up data obtained by Abdulkadir (2011) using an advanced non-intrusive tomographic measuring instrument called electrical capacitance tomography (ECT) was employed.

## **2.4 Void fraction**

The fraction of the channel volume that is occupied by the gas phase is described as void fraction. The void fraction ( $\epsilon$ ) is one of the most important parameters used to characterize two-phase flows. Void fraction could be measured by many methods such as quick-close valve,  $\gamma$  rays, x-rays, microwave, etc. ECT technology is prospectively useful because it is accurate, economical, non-intrusive, safe and fast. ECT is a kind of tomography process technology and provides a new way to solve the problems of void fraction measurement Li (2001).

However, it is a significant physical value for determining other numerous parameters such as two-phase flow viscosity and density. Void fraction data is also used for obtaining the relative average velocity of two-phases and also employed in models for predicting flow pattern transitions, heat transfer, interfacial area calculation and determination of pressure drop. In addition, literature reported various correlations for predicting void fraction and

classified them in terms of their method and physics involved in deriving these correlations as flow dependent or flow independent.

#### 2.4.1 Concept of void fraction

Void fraction is defined as the volume of space the gas phase occupies in a given two phase flow in a pipe- It is a key parameter which is used in estimating other parameters such as pressure drop, liquid holdup and heat transfer. In facilitating better understanding of void fraction, it is worthwhile to highlight some of the most common terminologies and definitions of parameters that would be encountered throughout this work. For a total pipe cross sectional area  $A$ ; the void fraction is given by

$$\varepsilon = \frac{A_G}{A} \dots \dots \dots (2.3)$$

Liquid holdup is the complement of the void fraction in the pipe; it is the remaining volume of space occupied by the liquid phase. Thus, liquid holdup is

$$H_L = 1 - \varepsilon = \frac{A_L}{A} \dots \dots \dots (2.4)$$

The quality of the mixture,  $X$ , in the isothermal flow case we are considering here is taken as the input mass of the gaseous phase to that of the total mixture mass of  $m$ , hence

$$X = \frac{M_G}{M_M} \dots \dots \dots (2.5)$$

The slip ratio,  $S$ , is defined as the ratio of the actual velocities between the phases. A slip ratio of unity for a mixture being the homogeneous case where it is assumed that both phases travel at the same velocity. The slip ratio is defined as

$$S = \frac{U_G}{U_L} \dots \dots \dots (2.6)$$

The superficial gas  $U_{SG}$ , and liquid  $U_{SL}$ , velocities are defined as the velocities of the gas or liquid phase in the pipe assuming the flow is a single phase in either gas or liquid respectively. From the definitions given above and writing conservation of mass for each phase and total flow, we can define the relationships,

$$U_G = \frac{U_{SG}}{\varepsilon} \dots \dots \dots (2.7)$$

$$U_L = \frac{U_{SL}}{1-\varepsilon} \dots \dots \dots (2.8)$$

$$\frac{X}{1-X} = \left(\frac{\rho_G}{\rho_L}\right) \left(\frac{U_{SG}}{U_{SL}}\right) \dots \dots \dots (2.9)$$

#### 2.4.2 Classification of void fraction

At a given point in the flow, the local fluid is either gas or one of the other phases. The probability of finding gas at a given point may be determined using local probes and is referred to as the local void fraction  $\varepsilon_{Local}$  - Hewitt et.al (1982). Thus  $\varepsilon_{Local} = 0$  means when liquid is present and  $\varepsilon_{Local} = 1$  when gas is present. Typically, the local time averaged void fraction cited, or measured using a miniature probe, which represents the fraction of time gas, was present at that location in the two-phase flow. If  $PK_{(r,t)}$  represents the local instantaneous presence of gas or not at some radius  $r$  from the channel at time  $t$ , then  $PK_{(r,t)} = 1$  when gas is present and  $PK_{(r,t)} = 0$  when liquid is present. Thus, the local time-averaged void fraction is defined as

$$\varepsilon_{local(r,t)} = \frac{1}{t} \int PK(r, t) dt \dots \dots \dots (2.10)$$

The chordal void fraction  $\varepsilon_{chordal}$  is typically measured by shining a narrow radioactive beam through a channel with a two phase flow inside, calibrating its different absorptions by the vapor



and liquid phases, and then measuring the intensity of the beam on the opposite side, from which the fractional length of the path through the channel occupied by the vapor phase can be determined. The chordal void fraction is defined as

$$\epsilon_{chordal} = \frac{L_G}{L_G + L_L} \dots \dots \dots (2.11)$$

Where  $L_G$  is the length of the line through the gas phase and  $L_L$  is the length through the liquid phase” Thome (2004).

The cross- sectional void fraction  $\epsilon_{c-s}$  is typically measured using either an optical means or by an indirect approach, such as the electrical capacitance of a conducting liquid phase. Also, it is the most widely used void fraction definition known as cross-sectional average void fraction which is based on the relative cross-sectional areas occupied by the respective phases.

The cross-sectional void fraction is defined as

$$\epsilon_{c-s} = \frac{A_G}{A_G + A_L} \dots \dots \dots (2.12)$$

Where  $A_G$  is the area of the cross-section occupied by the vapor phase and  $A_L$  is that of the liquid -Thome (2004).

Another measure is the volume-averaged void fraction. This can be interpreted as the fraction of volume of the reference volume occupied by the gas phase at time (t). The volumetric void fraction  $\epsilon_{vol}$  is typically measured using a pair of quick-closing valves installed along a channel to trap the two-phase fluid, whose respective gas and liquid volumes are then determined. The volumetric void fraction can be represented as

$$\epsilon_{vol} = \frac{V_G}{V_G + V_L} \dots \dots \dots (2.13)$$

Quality (x) of a two-phase flow is defined as the ratio of the gas mass flow rate to the total mass flow rate but sometimes confused with void fraction definition. The quality is expressed in terms of mass and is a function of the phase density and void fraction. The quality (x) is given by

$$X = \frac{W_G}{W_G + W_L} = \frac{W_G}{W} \dots \dots \dots (2.14)$$

“However, another important definition in two -phase flow also confused with void fraction is the gas volumetric flow fraction denoted as  $\beta$ . It refers to the ratio of the gas volumetric flow rate over the mixture volumetric flow rate given by

$$\beta = \frac{Q_G}{Q_G + Q_L} = \frac{Q_G}{Q} \dots \dots \dots (2.15)$$

Where  $Q_G$  . and  $Q_L$  - are the volumetric flow rates of liquid and gas respectively.

The major difference between void fraction and gas volumetric flow fraction is that, in void fraction, there is slippage in two- phase flow due to density difference whiles the later assumes that both phases move with the same velocity and hence known as void fraction in the homogeneous flow” Thome (2004).

### 2.4.3 The measurement principle

Void fraction can be measured by measuring the changes of material properties owing to the presence or absence of the gas. Some of the properties that can be used for checking the presence of gas and the corresponding sensors are as follows:

- Electrical impedance
- Impedance probe
- Refractive index
- Optical probes

- Density-(absorption coefficient)
- X-rays or gamma ray densitometers

## 2.5 Void fraction correlations for inclined pipes

The majority of the correlations developed for void fraction are for horizontal with very few for other inclination angles, the common one being upward. Categorizing the correlations along their applicability with regard to angle of inclination would not serve any purpose as most of them would fall under the horizontal case. Most of the data from which the correlations have been developed were from small pipe diameters, short length pipes in a laboratory setting with controlled, and relatively small mass flow rates while mixtures of air-water dominate with regard to the fluids considered Woldesemayat et al. (2007).

The correlation of Guzhov et al. (1967) which can handle the plug and stratified flow regimes in pipes with small inclination angles to the horizontal ( $\pm 9^\circ$ ) is also considered here. The correlation is a function of the homogeneous void fraction and the mixture Froude number.

$$\varepsilon = 0.81_{\varepsilon_H} \left( 1 - \exp(-2.2\sqrt{F_r}) \right) \dots \dots \dots (2.16)$$

Greskovich and Cooper (1975) developed a correlation from air- water data for inclined flows. It was noted that the data showed little diameter dependency above 2.54-cm but was considerably dependent on inclination angles.

$$\varepsilon = \frac{1}{\left[ 1 + 0.671 \left( \frac{(\sin \theta)}{F_r^{0.5}} \right) \right]} \varepsilon_H \dots \dots \dots (2.17)$$

A general type of correlation given in a plot format by Flanigan-(1958) put into equation form by the AGA (American Gas Association) is considered. The correlation assumes that pipe inclination has no effect on void fraction and that it is only a function of gas superficial velocity. Gomez et al.(2000) developed a correlation for predicting liquid holdup for slug flow for horizontal, inclined and vertical orientations. The data covers pipe diameters between 5.1 – 20.3 inches and the fluids considered were air, nitrogen, freon, water and kerosene. The liquid slug is seen to be dependent on the inclination angle, mixture velocity and viscosity of the liquid phase. They claimed surface tension has no significant effect on the holdup in comparison to the viscosity of the liquid. The equation is of the form

$$\varepsilon = 1 - e^{-(0.45\theta + 2.48 \cdot 10^{-6} Re_M)} \dots \dots \dots (2.18)$$

**2.6 Drift flux correlations**

This type of correlations are based on the work of Zuber and Findlay (1965) where the void fraction can be predicted taking into consideration the non-uniformity in flows and the difference in velocity between the two phases. This model is good for any flow regime. It has the general expression given by

$$\varepsilon = \frac{U_{SG}}{C_o U_M + U_{GM}} \dots \dots \dots (2.19)$$

Where-  $C_o$  is the distribution parameter and  $U_{GM} = U_G - U_M$  is the drift velocity.

Kokal and Stanislav-(1989) correlated their air-oil experimental data in horizontal and near horizontal ( $\pm 9^\circ$ ) pipe using the drift flux relation and recommended their correlation for all flow regimes. It is given as

$$\varepsilon = \frac{U_{SG}}{1.2U_M + 0.345 \left[ \frac{gD(\rho_L - \rho_G)}{\rho_L} \right]^{1/2}} \dots \dots \dots (2.20)$$

## 2.7 Pressure drop in two-phase inclined pipes

The ultimate goal in two-phase flow models is to calculate the total pressure drop that occurs in a two-phase flow system. The knowledge of pressure drop in a two-phase flow system is important for its design. It enables the designer to size the pump required for the operation of the flow system. The total pressure drop calculations along horizontal pipe consist of two components- the acceleration pressure drop in the mixing zone and the frictional pressure drop in the slug body.

In this work, the modified Beggs and Brill correlation stated below is used to calculate the pressure drop along the entire 6 meters pipe using experimental data - The general pressure drop equation is given as

$$-\frac{dp}{dz} = \frac{g \sin \theta}{g_c} (\rho_L H_L + \rho_G (1 - H_L)) + \frac{f_m U_m^2 \rho_m}{2g_c d} + \frac{f_m U_m dU_m}{g_c dZ} \dots \dots \dots (2.21)$$

Where  $g_c$  is a conversion factor to oil field unit

Whilst the new definition of the two-phase friction factor by Beggs and Brill (1957) is given by the following expression

$$\frac{1}{\sqrt{f_m}} = -2 \log \left[ \frac{\varepsilon}{3.7065d} - \frac{5.0452}{R_{em}} \log \left( \frac{1}{2.8257} \left( \frac{\varepsilon}{d} \right)^{1.1098} \frac{5.8506}{(R_{em})^{0.8981}} \right) \right] \dots \dots (2.22)$$

Where " $\varepsilon$ " is the surface roughness,  $R_{em}$  is the mixture Reynolds number which can be calculated using the following relation.

$$R_{em} = \frac{\rho_m U_m D}{\mu_m} \dots \dots \dots (2.23)$$

As mostly stated in literature, mixture density and mixture viscosity are

$$\rho_m = \rho_L H_L + (1 - H_L) \rho_G \dots \dots \dots (2.24)$$

$$\mu_m = \mu_L H_L + (1 - H_L)\mu_G \dots \dots \dots (2.25)$$

After the calculation of the necessary parameters, the gravitational, frictional and accelerational pressure drops are calculated from which representative results in the form of graphs are presented in chapter four.

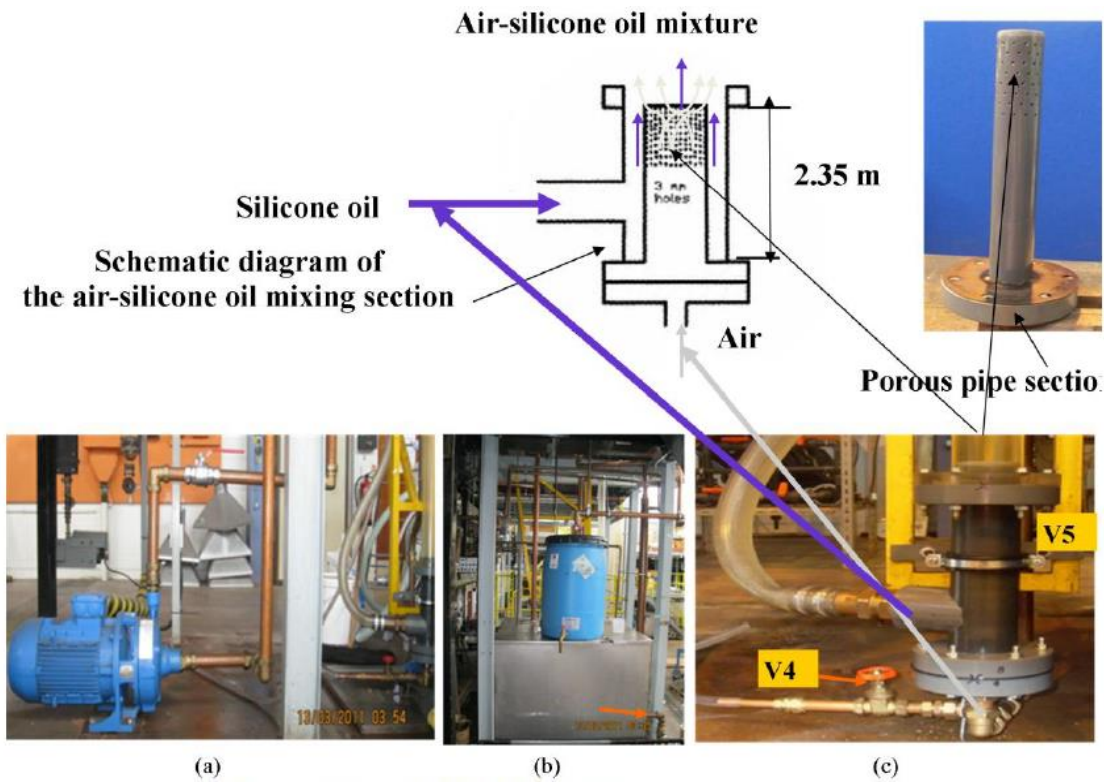
## Chapter 3

### DATA ACQUISITION SETUP

This chapter presents a summary of the data obtained from a series two-phase air-silicone oil flow experiment carried out on an inclinable rig by Abdulkadir (2011) at the L3 Laboratories of the department of chemical and environmental engineering at the University of Nottingham. An overview of the experimental facility, test fluids and capability of the flow facility presented.

#### 3.1 Overview of the experimental facility

The experimental work was carried out on an inclinable pipe flow rig as shown in figure 3.1 and 3.2. The details of the experiment can be found in Abdulkadir (2011). Data collected from the experiments was done at laboratory temperature of 200°C and 1 bar of atmospheric pressure with the physical properties of the working fluids shown in table 3.1.



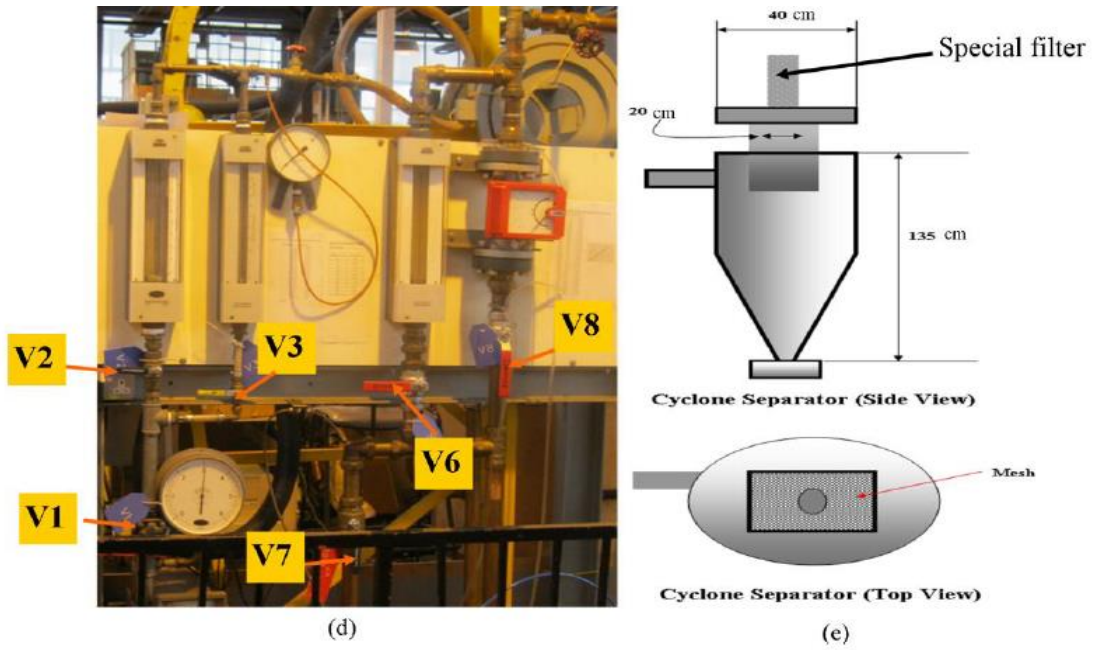


**Figure 3.1** The components of the rig (a) liquid pump (b) liquid tank (c) air-silicone oil mixing section (d) rotameters and (e) cyclone separator Abdulkadir (2011)





**Figure 3.2 Experimental flow facility Abdulkadir (2011b)**

### **3.2 System (test fluid)**

The air-silicone oil system was selected for the reasons listed below (**Abdulkadir, 2011b**)

- It is not toxic, hence environmentally friendly, and reasonably less expensive.
- It has thermal stability and transfer qualities - at both hot and cold extremes
- It is fire resistant
- It has good electrical insulation property
- It has no; odour, taste or chemical transference
- It is easily detected in acrylic pipe
- There are several proven techniques for its use and advanced instrumentation for liquid holdup or void fraction measurements.

**Table 3.1 Physical properties of air/silicon**

<b>Fluid</b>	<b>Viscosity</b> (kgm <sup>-1</sup> s <sup>-1</sup> )	<b>Density</b> (Kgm <sup>-3</sup> )	<b>Surface Tension</b> (Nm-1)	<b>Thermal Conductivity</b> (Wm <sup>-1</sup> K <sup>-1</sup> )
<b>Air</b>	0.000018	1.18	0.02	0.1
<b>Silicone Oil</b>	0.00525	900		

Abdulkadir (2011b)

### 3.3 Parameters determined for this present study

In this present work the method of determination of characterization parameters presented by Abdulkadir *et al.* (2014) is adopted. With the ECT data the following parameters were calculated

- Lengths of Taylor bubbles and liquid slugs
- Slug frequencies,
- The velocities of Taylor bubbles and liquid slugs
- Void fractions within the Taylor bubbles and liquid slugs

#### 3.3.1 Translational or rise velocity of Taylor bubble (structure velocity)

Fundamentally translational velocity is given by

$$U_N = \frac{\Delta L}{\Delta t} \dots \dots \dots (3.1)$$

Where  $\Delta L$  = the distance between the two ECT planes and  $\Delta t$  =time taken for the individual slugs to travel between the two planes.

### 3.3.2 Determination of the distance ( $\Delta L$ ) between the two ECT planes

The planes are located at 4.4 m and 4.489 m above the mixer section at the base of the riser.

$$\Delta L = 4.489m - 4.4m = 0.089m \dots \dots \dots (3.2)$$

### 3.3.3 Determination of time delay

As the individual slugs pass between the two ECT planes as shown in figure 3.3, the time taken to reach the planes are recorded in the form of time series wave output signals. Cross correlating between these two signals gives the time delay a slug travels between the planes. Cross correlation for two linearly dependent time series, a and b is the average product of,  $a - \mu_a$  and  $b - \mu_b$ . Where  $\mu_a$  and  $\mu_b$  are the mean of time series a, and b respectively. This average product is the co-variance of a and b in the limit as the sample approaches infinity. Hence for any time delay  $\tau$ , the co-variance function between a (t) and b(t) is :  $C_{ab} = E[\{a(t) - \mu_a\}\{b(t + \tau) - \mu_b\}]$

$$= \lim \frac{1}{T} \int_0^T [\{a(t) - \mu_a\}\{b(t + \tau) - \mu_b\}] dt = R_{ab}(\tau) - \mu_a \mu_b \dots \dots \dots (3.3)$$

Where

$$R_{ab} = \lim \frac{1}{T} \int_0^T a(t) b(t + \tau) dt \dots \dots \dots (3.4)$$

The correlation co-efficient is defined as follows

$$\rho_{ab}(\tau) = \frac{C_{ab}(\tau)}{\sqrt{C_{aa}(0)C_{bb}(0)}} = \frac{R_{ab}(\tau) - \mu_a \mu_b}{\sqrt{(R_{aa}(0) - \mu_a^2)(R_{bb} - \mu_b^2)}} \dots \dots \dots (3.5)$$

These equations have been programmed as computational macro programme to determine the structure velocity of the liquid slug body, (Abdul-kadir *et al.* 2014).

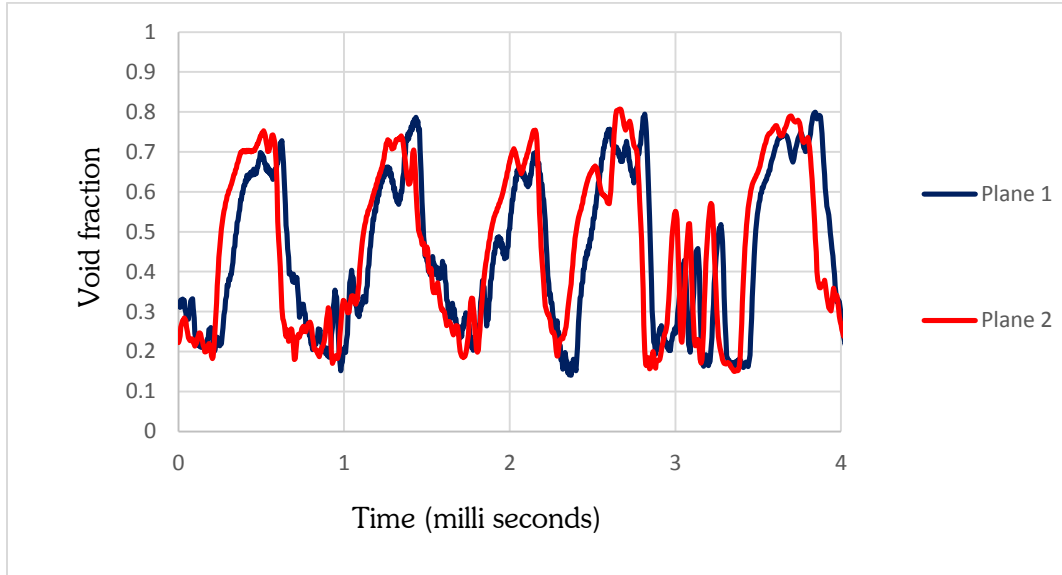


**Figure 3.3 Void fraction time series from the two ECT probes**

### 3.3.4 Slug frequency

This is the number of slugs passing through a defined pipe cross-section in a given time period.

The power spectral density approach (PSD) defined by Bendat and Piersol (1980) was used. PSD basically measures how the power in a signal changes over frequency. It is defined mathematically as the Fourier transform of an auto-correlation sequence. The PSD function is defined as follows

$$S_{ab}(f) = \int_{-\infty}^{+\infty} R_{ab}(\tau) e^{-j2f\tau} d\tau \dots \dots \dots (3.6)$$

### 3.3.5 Lengths of the slug unit, the Taylor bubble and the liquid slug

From the relation  $U_N = \frac{L_{SU}}{\theta}$  where  $L_{SU}$  is the length of slug unit,  $\theta$  is the time for a particular slug to pass the probe. But frequency  $\theta = \frac{1}{f}$  ..... (3.7)

Therefore  $L_{SU} = \frac{U_N}{f}$  ..... (3.8)

The length of slug unit is therefore calculated from equation (3.8)

Again for an individual slug unit, assuming steady state so that the front and back of the slug have the same velocity

$$L_{SUi} = Kt_{SUi} \dots \dots \dots (3.9)$$

$$L_{TBi} = U_{Ni}t_{TBi} \dots \dots \dots (3.10)$$

$$L_{Si} = U_{Ni}t_{Si} \dots \dots \dots (3.11)$$

Dividing equation (3.10) by equation (3.11) results in the following expression

$$\frac{L_{TBi}}{L_{Si}} = \frac{Kt_{TBi}}{Kt_{Si}} = Z \dots \dots \dots (3.12)$$

$$L_{TBi} = ZL_{Si} \dots \dots \dots (3.13)$$

But

$$L_{SUi} = L_{TBi} + L_{Si} \dots \dots \dots (3.14)$$

Finally, substituting equation (3.13) into equation (3.14) and re-arranging results in the following expressions

$$L_{Si} = \frac{L_{SUi}}{Z + 1} \dots \dots \dots (3.15)$$

$$L_{TBi} = L_{SUi} - L_{Si} \dots \dots \dots (3.16)$$

The lengths of the liquid slug and Taylor bubble are estimated from equation (3.15) and equation (3.16) respectively.

### 3.4 Summary

This chapter has presented both the experimental facility and instrumentation used for measurements. It also includes the parameters that were needed in the analysis and discussion. The ensuing chapter deals with the processing of new raw data into required parameters and analysis of the results.

## CHAPTER 4

### RESULTS AND DISCUSSION

#### 4.1 Analysis of length; liquid slug, Taylor bubble and slug unit

The measured velocities and slug frequencies, the mean length of each Taylor bubble, liquid slug and slug unit are presented here. The lengths of liquid slug and slug unit can be observed to increase as the gas superficial velocity increases, for a constant liquid superficial velocity for both the  $0^\circ$  and  $30^\circ$  pipe inclination angles. However, at lower constant liquid superficial velocities of 0.05 and 0.09-m/s the increment is not high in both the length of liquid slug and slug unit as shown in figures 4.1 and 4.2. It is interesting to notice that as gas superficial velocity increases to 2.14- m/s at both liquid superficial velocities of 0.28- m/s and 0.38- m/s both the  $0^\circ$  and  $30^\circ$  has the same- lengths of liquid slug and slug unit. But on the other hand, the length of the Taylor bubble did not depict the same trend as gas superficial velocity increases as shown in figure 4.1.

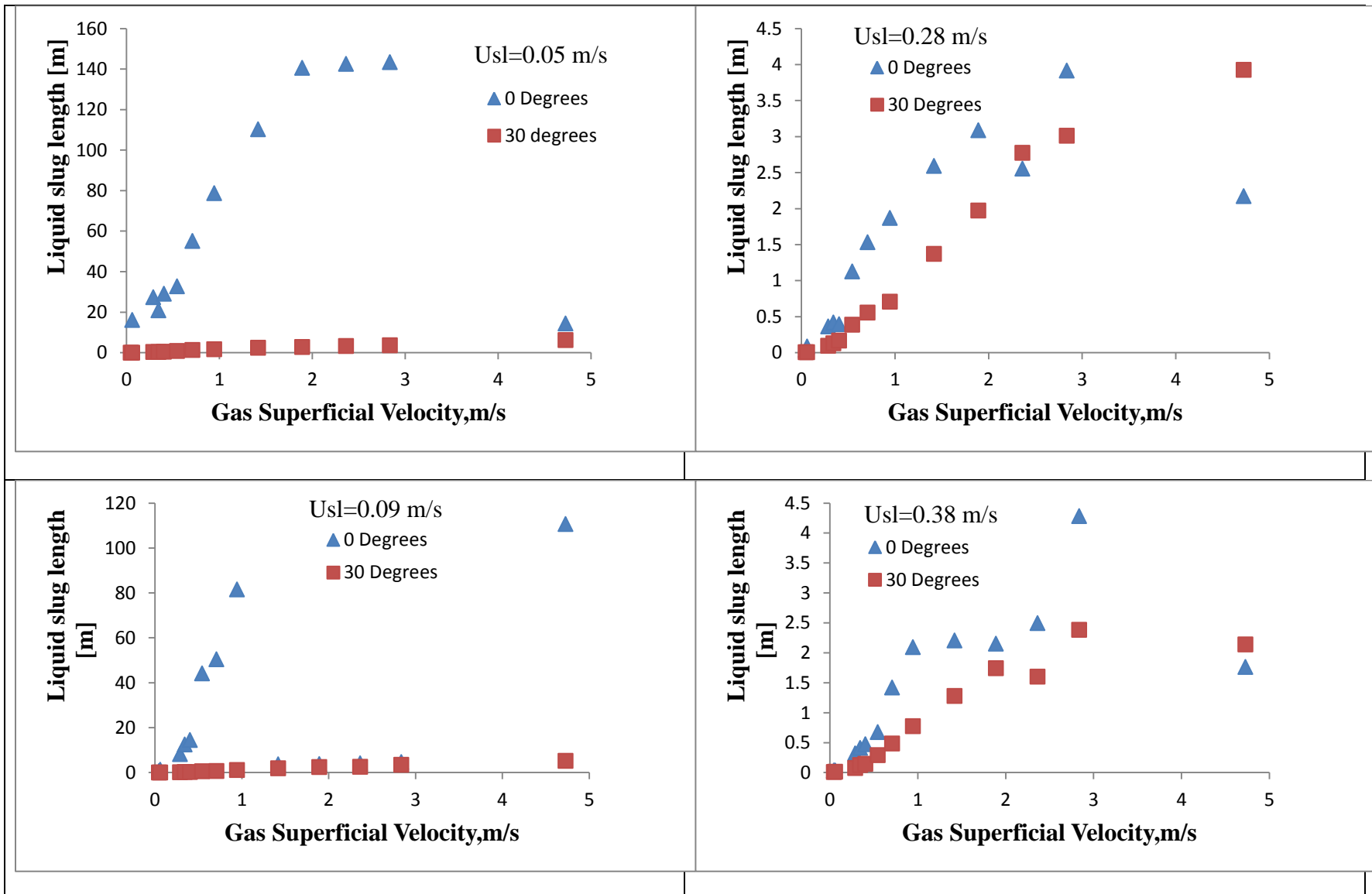


Figure 4.1 a plot of length of liquid slug against gas superficial velocity for various liquid superficial velocities



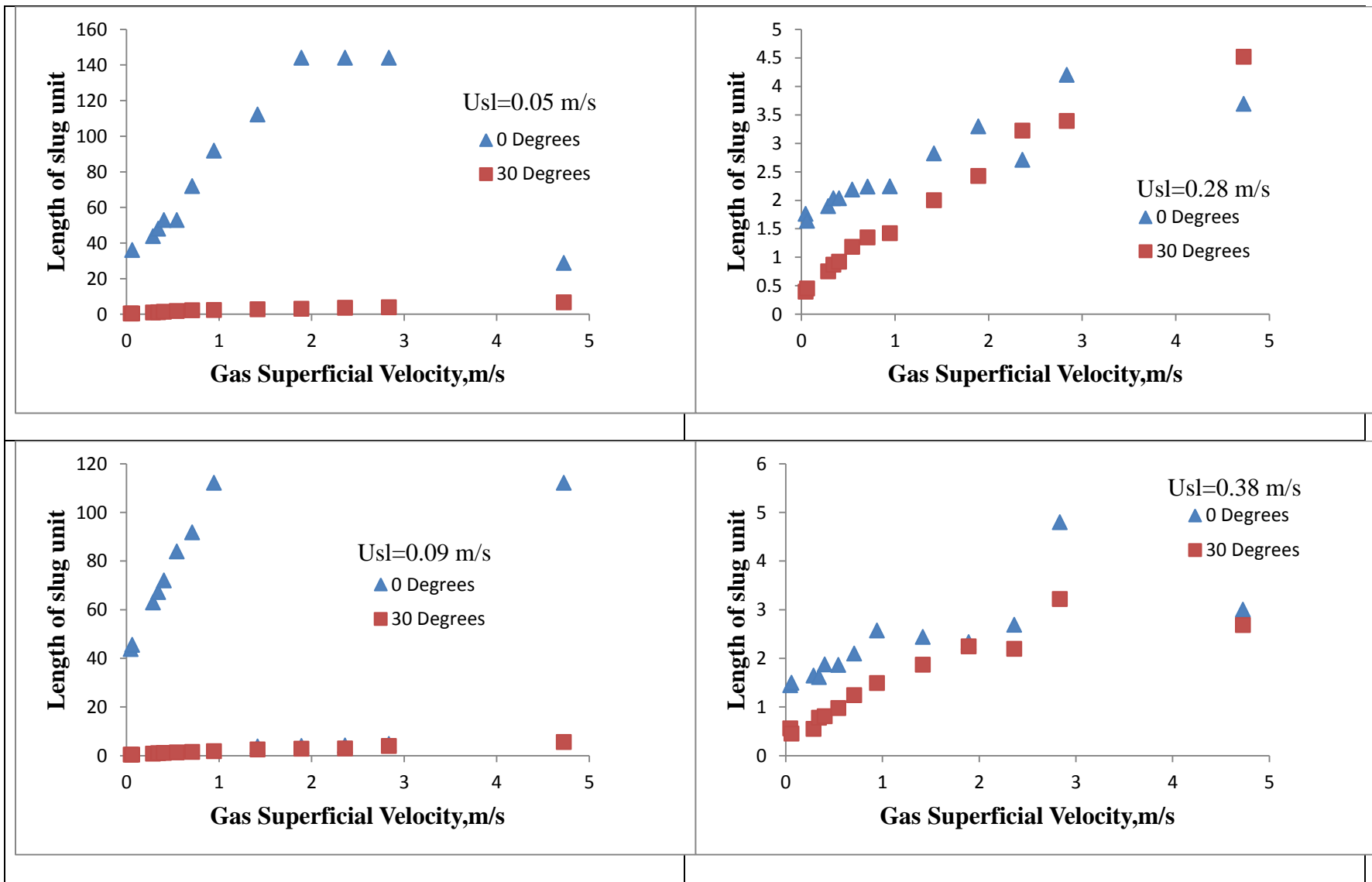


Figure 4.2 a plot of length of slug unit against gas superficial velocity for various liquid superficial velocities

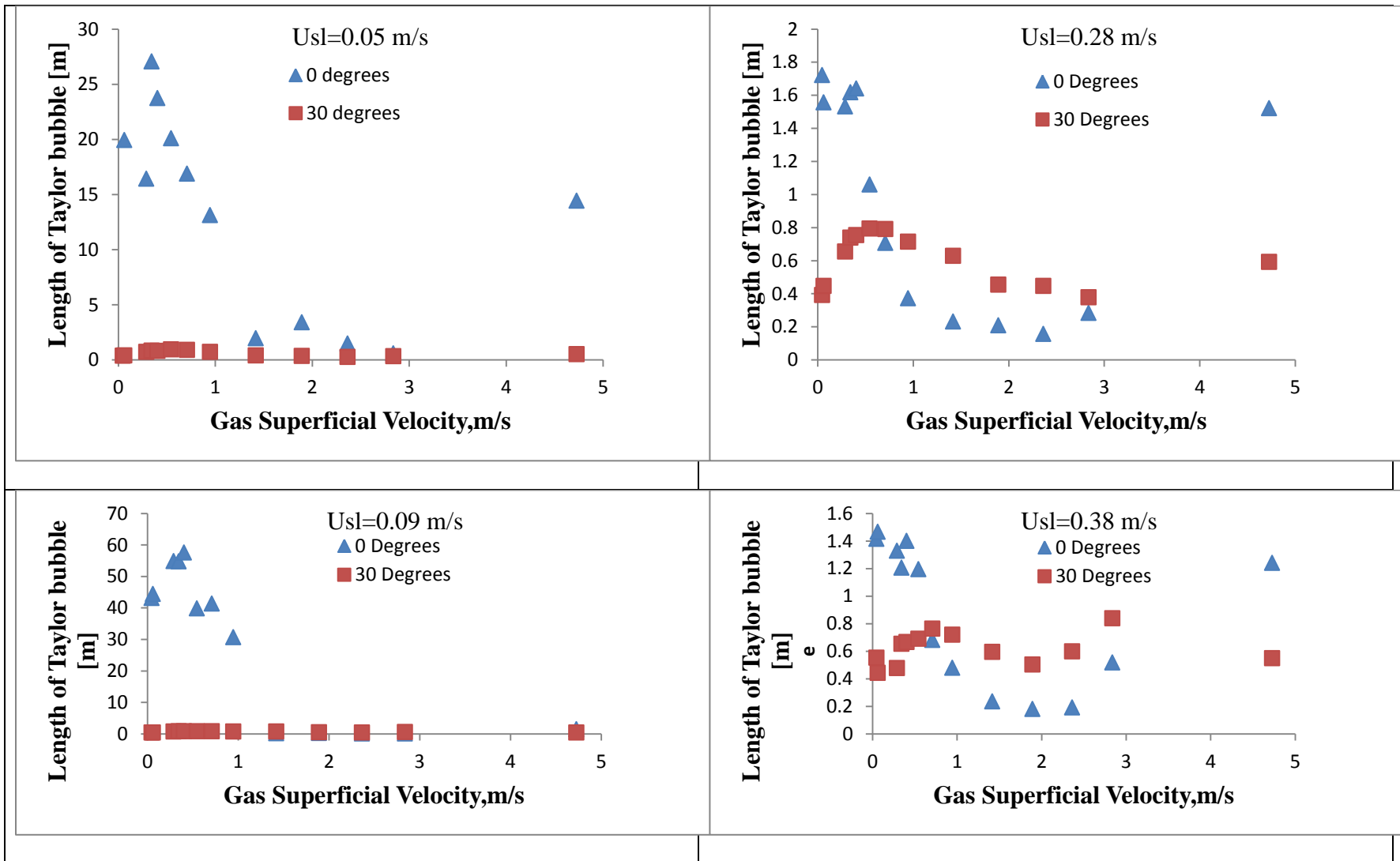


Figure 4.3 a plot of length of Taylor bubble against gas superficial velocity for various liquid superficial velocities

It can be concluded therefore that at a given liquid flow rate, a strong relationship exist between the plot of lengths of liquid slug and slug unit against the gas superficial velocity for  $0^\circ$  pipe inclination angle but the relationship is not as strong as in  $30^\circ$  pipe inclination at lower liquid flow rate. However, when the gas superficial velocity increases, there is a corresponding proportional increase in lengths of liquid slug and slug unit at both higher liquid flow rate of 0.38-m/s and this may be attributed to an increase in bubble coalescence as a result of increasing gas flow rate. The length of the Taylor bubble was observed to reduce with an increase in gas superficial velocity for the  $0^\circ$  pipe inclination at all liquid flow rate considered not the same in the case of  $30^\circ$  pipe inclination angle. The above observation can be explained by the fact that, the frequency of the slugging upsurges with increasing gas superficial velocity. Also for a given flow condition, the slug length keeps fluctuating as a result of continuous interaction between the phases at the tail of the Taylor bubble. The above conclusions are similar to observation reported by Hernandez-Perez (2008) and Abdulkadir (2011).

#### **4.2 Time and space average analysis**

The ECT used in the experiment provides data that is resolved in time and about a cross-section with several levels of averaging in time and space. The mean void fraction is obtained from the liquid hold up and then by averaging the time series data from the ECT. The time and space averaged information results in a liquid holdup which is widely used in many engineering estimation of pressure drop, void fraction, interfacial area calculation and heat transfer. Figure 4.4 shows a plot of mean void fraction against gas superficial velocity for air/silicone at an angle of inclination of  $0^\circ$  and  $30^\circ$  for various liquid and gas superficial velocities. The figure shows that, at liquid superficial velocity of 0.05-m/s, the mean void fraction begins from 0.37 at a gas superficial velocity of 0.047-m/s extending to a maximum

value of 0.734 at gas superficial velocity of 4.727-m/s for an inclination of  $0^\circ$ . On the other hand, for the  $30^\circ$  pipe inclination, the average void fraction begins at 0.074 extending to a maximum value of 0.818 at gas superficial velocity of 4.727-m/s. It can be concluded therefore that an increase in pipe inclination from  $0^\circ$  to  $30^\circ$  brings about a corresponding reduction in average void fraction. However, the observed trend changes as the gas superficial velocity increases from 2.886 m/s thereby causing the  $0^\circ$  inclination to have a lower average void fraction-In addition, for liquid superficial velocities of 0.09, 0.28 and 0.38-m/s, the initial average void fractions begins at - 0.08, 0.669 and 0.062, respectively for the  $0^\circ$  inclination whereas it starts at 0.0576, 0.423, and 0.0404, respectively for the  $30^\circ$  pipe inclination. This observed trend is similar to what is obtainable for the  $0^\circ$  pipe inclination at a liquid superficial velocity of 0.05- m/s where a decrease in average void fraction at the higher gas superficial velocity is seen. It can be concluded from the plots that, the trend of mean void fractions is the same for all the inclinations considered for this work. This may be due to the fact that an increase in the gas superficial velocity may increase bubble population there by bringing about an increase in average void fraction. The statement above confirms the conclusions of Hernandez-Perez et al. (2010) that the average void fraction distribution is strongly affected by pipe inclination, but does not strongly affect the bubble size distribution.

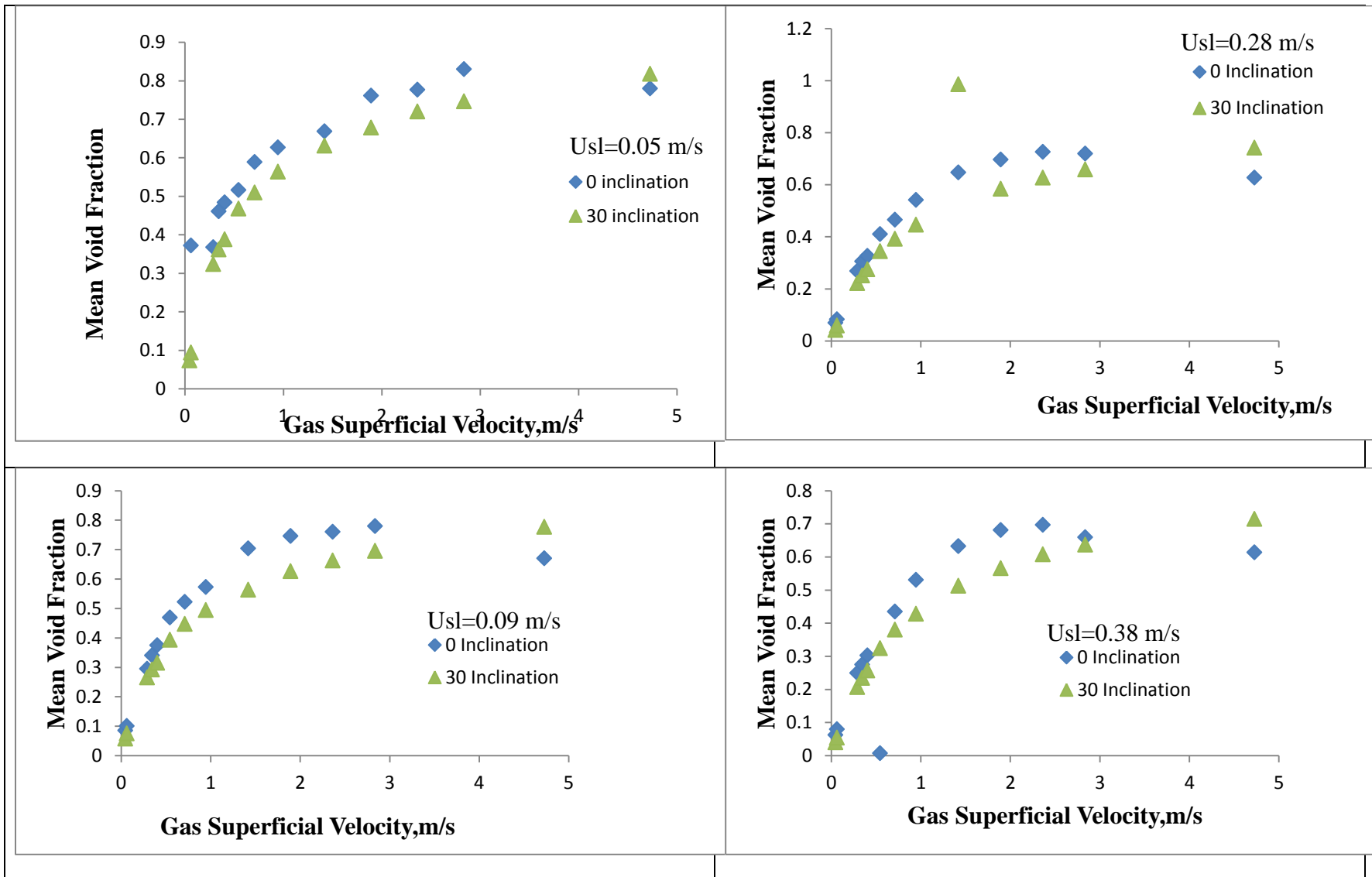
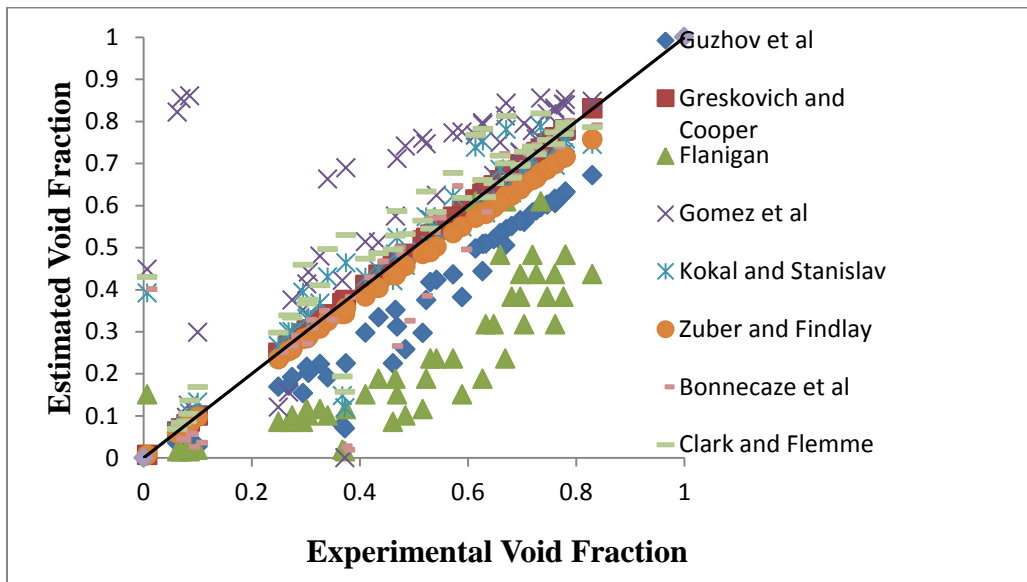


Figure 4.4 Effect of gas superficial velocity and angle of inclination on average void fraction at different liquid superficial velocity

#### 4.2.1 Mean void fraction from empirical correlations

This section deals with estimation of average void fraction using empirical correlations which are mostly employed in the industry. Figure 4.5(a) and (b) shows a comparison of experimental ECT data with empirical models reported in literature. The empirical models considered are as follows- Guzhov et al.(2000), Greskovich & Cooper (1975), Flanigan (1958) , Gomez et al (2000), Kokal & Stanislav (1989), Zuber and Findlay (1965), Flanigan (1958) , Bonnecaze et al.(1971) and Clark &Flemmer (1985) .



**Figure 4.5 (a) Experimental void fraction against empirical models for the 0° inclination**

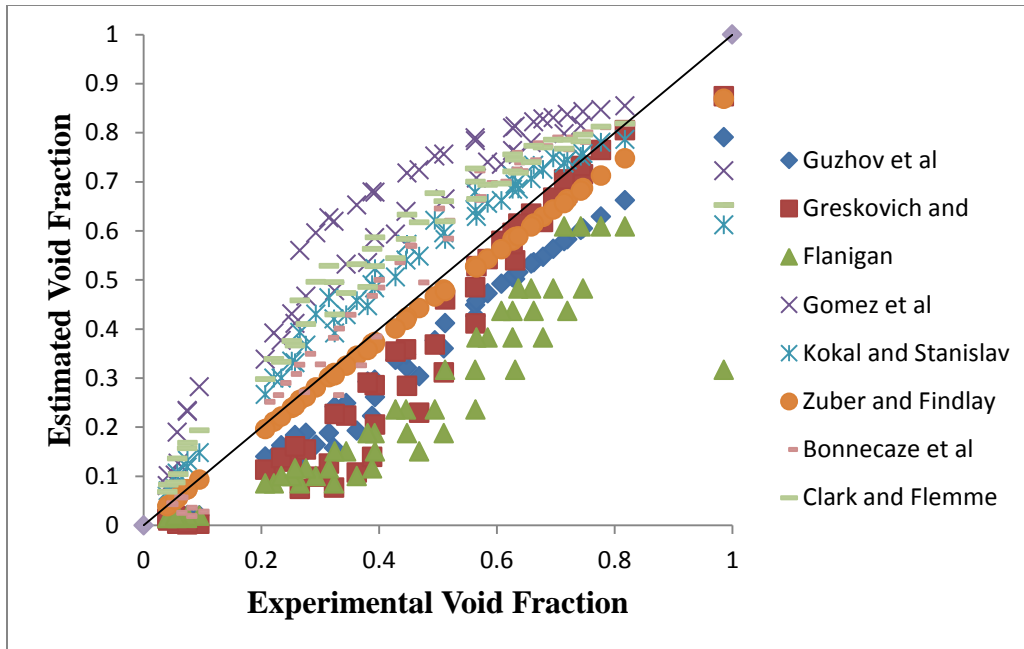


**Figure 4.5 (b) Experimental void fraction against empirical models for the 30° inclination**

The mathematical relation used to estimate Average Root Mean Square (ARMS) is given by

$$ARMS = \sqrt{\frac{1}{n} \sum_{i=1}^n e_i^2} \dots \dots \dots (4.1)$$

ARMS measure the data dispersion around zero deviation, in which; e is the difference between experimental and estimated data.

$$e_i = [\varepsilon_{exp} - \varepsilon_{est}] \dots \dots \dots (4.2)$$

**Table 4.1 Average root mean square (ARMS) of empirical correlation for the 0° and 30° pipe inclination angles**

<b>Correlation</b>	<b>0°</b>	<b>30°</b>
Guzhov et al. (1967)	4.31	10.58
Greskovich and Cooper (1975)	6.64	13.95
Flanigan(1958)	5.02	6.09
Gomez et al.(2000)	11.17	23.24
Kokal and Stanislav(1989)	6.25	22.44
Zuber and Findlay (1965)	5.04	15.54
Bonnecaze et al.	7.92	23.59
Clark and Flemme	7.67	26.41

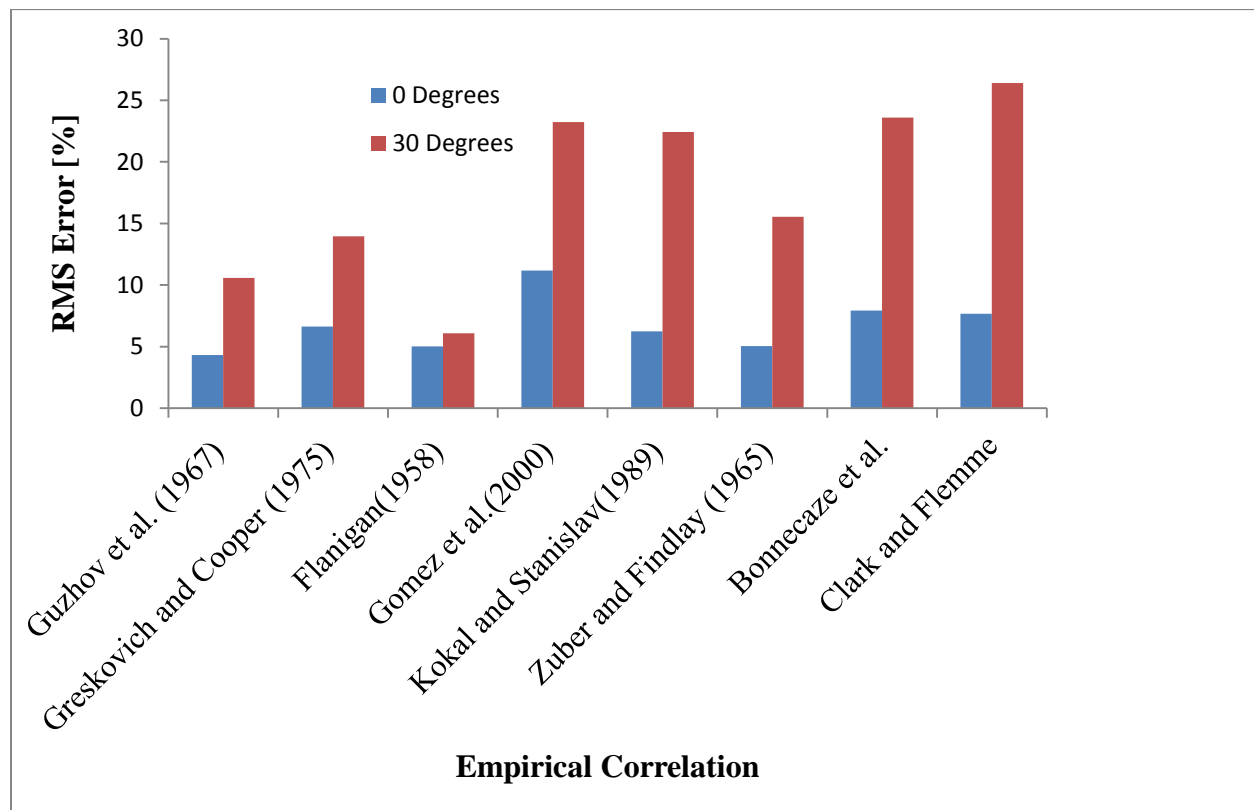


**Figure 4.6** RMS of empirical correlation



The correlations used are based on the drift-flux model explained in detail in Chapter two. It is interesting to know that there is no particular correlation that gave better results in the two inclination angles considered in this work. It is worth mentioning that a general type correlation given by Flanigan-(1958) assumes that pipe inclination has no effect on average void fraction.- However, as can be noticed from Table 4.1 the RMS values are 5.02-% and 6.09-%, respectively for the inclination angles considered. Most of the correlations that are used in the industry does not take into consideration pipe inclination. The very few that take into consideration angle of inclination are Greskovich and Cooper (1975) and Gomez et al. (2000). It is however interesting to know that for the Greskovich and Cooper (1975) correlation the RMS is lower for 0° inclination and then increases to 13.95-% for the 30° inclination angle. These deductions can be attributed to the conditions under which the researcher's experiments were performed. However, the general correlation given by Zuber and Findlay (1965), Kokal and Stanislav (1989) gave a good results for the 0° inclination.-This can be likened to the various conditions under which each of the researchers conducted their experiment. Though these correlations- did not take into consideration angle of inclination but rather drift flux.

### **4.3 Void fraction analysis**

Void fraction ( $\epsilon$ ) is an important parameter to characterize two phase flow. It is used to determine parameters such as two-phase density, two-phase viscosity, and average velocity among others. It can be seen from figure 4.7 that the void fraction in the liquid slug is directly proportional to the gas superficial velocity for a constant liquid superficial velocity for both 0° and 30° pipe inclination angles. However at 2.4-m/s, gas superficial velocity both 0° and 30° pipe inclination angles have the same average void fraction in the liquid slug. This may be due to the fact that any increase in the gas flow rate may increase bubble formation, hence causing an

increase in the average void fraction. This is a confirmation made by researchers like Nicklin et al. (1962) and Mao and Dukler (1991). On the other hand, the liquid flow rate has a minimal influence on the void fraction in the liquid slug. In the case of the void fraction in the Taylor bubble it can be seen from figure 4.8 that the void fraction in the Taylor bubble increases as the gas velocity increases for both  $0^\circ$  and  $30^\circ$  pipe inclination angles. It was noted that, the void fraction in the Taylor bubble fluctuates in both  $0^\circ$  and  $30^\circ$  pipe inclination for all the liquid superficial velocities considered. It was also observed that, increasing gas flow rate resulted in more bubbles formation in the liquid slug, which may eventually coalesce with the Taylor bubble hence increases its void fraction. It is worthy of mention that a decrease in void fraction may occur when there is a collapse of Taylor bubble signifying a transition to a spherical cap bubble.

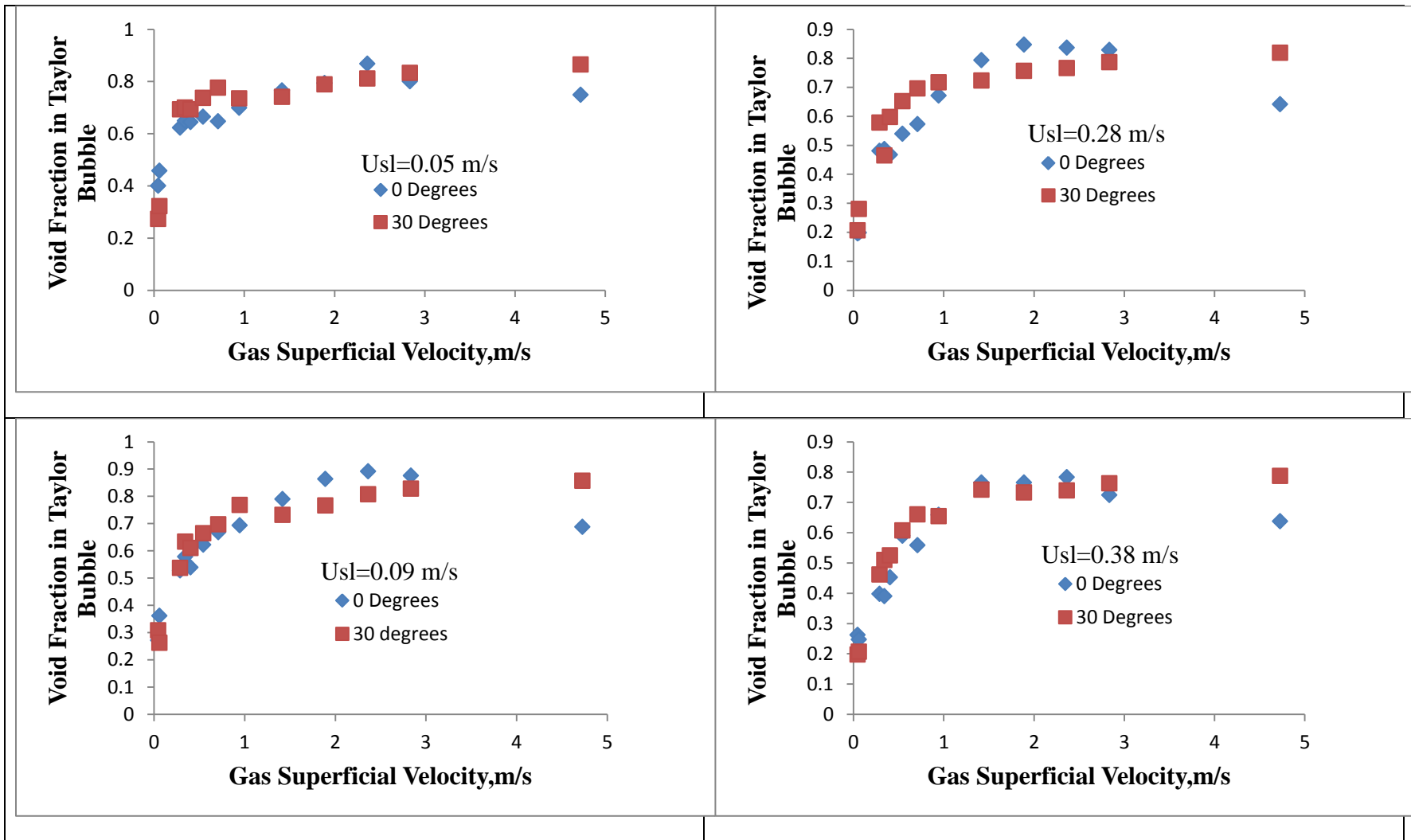


Figure 4.7 a plot of void fractions in the Taylor bubbles against gas superficial velocity for various liquid superficial velocities

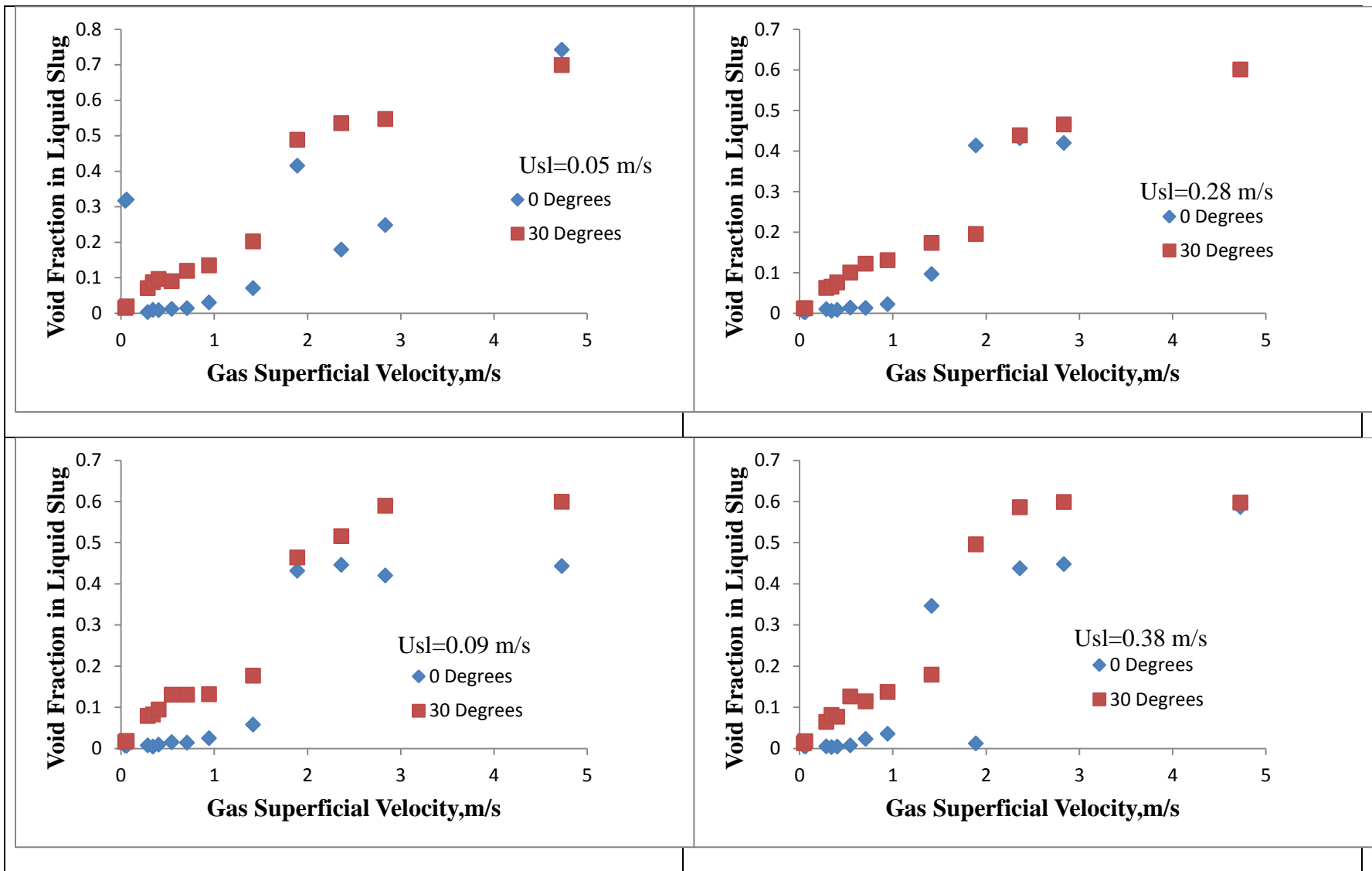


Figure 4.8 a plot of void fractions in the liquid slug against gas superficial velocity for various liquid superficial velocities

#### **4.4 Pressure drop**

Pressure drop is an important parameter in pipeline design. It is an essential variable for the determination of the pumping energy for a given flow. The diversity of techniques used by different authors to present two-phase flow pressure drop indicates, that pressure drop in two-phase flow can depend on a significant number of variables such as gravity. The effect of gravity on pressure drop is intuitive. Figure 4.9 and 4.10 shows a plot of frictional, accelerational and gravitational pressure gradients for  $0^\circ$  and  $30^\circ$  pipe inclination angles determined using the Beggs and Brill (1973) correlation.

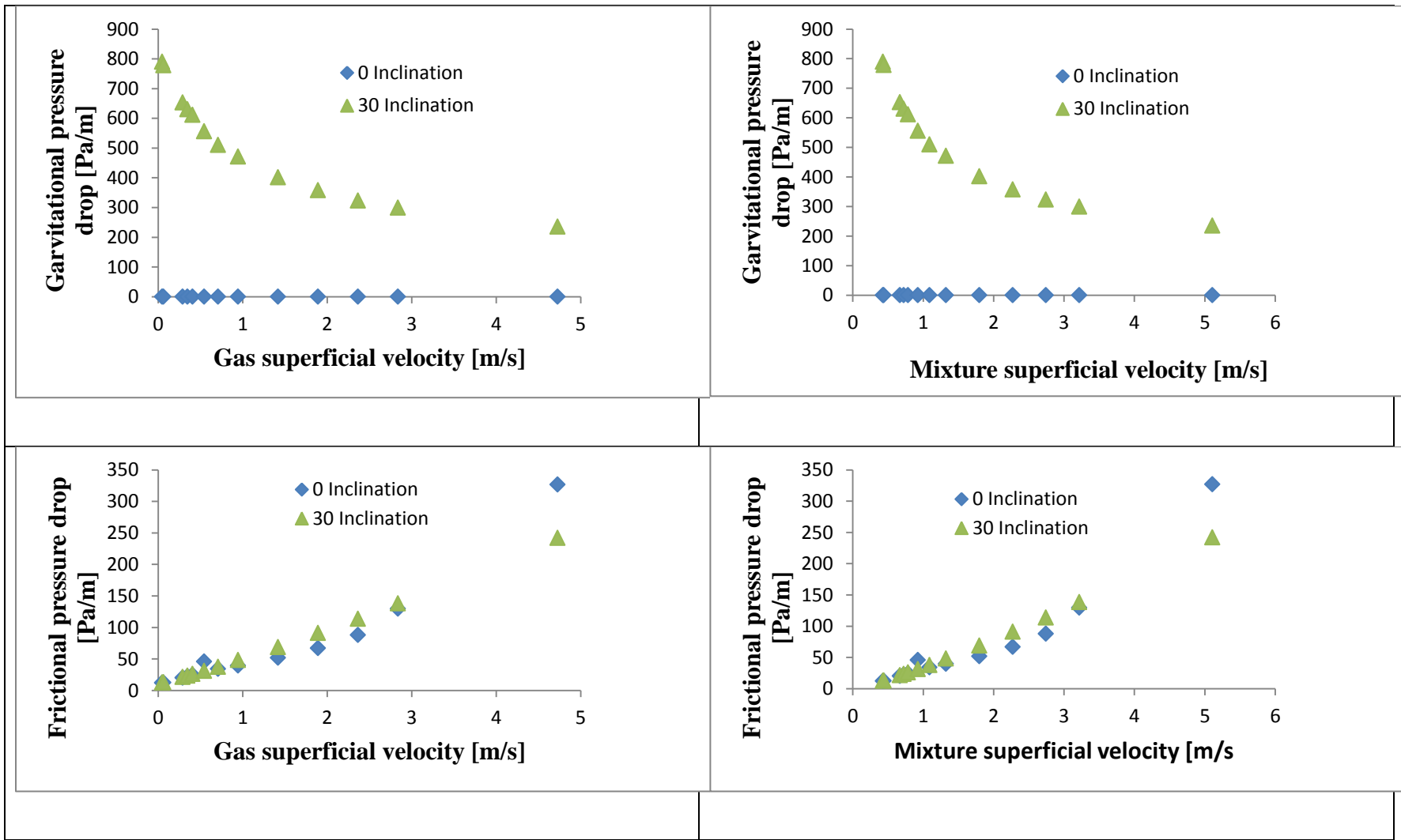


Figure 4.9 Influence of gas superficial velocity on gravitational and frictional pressure gradient

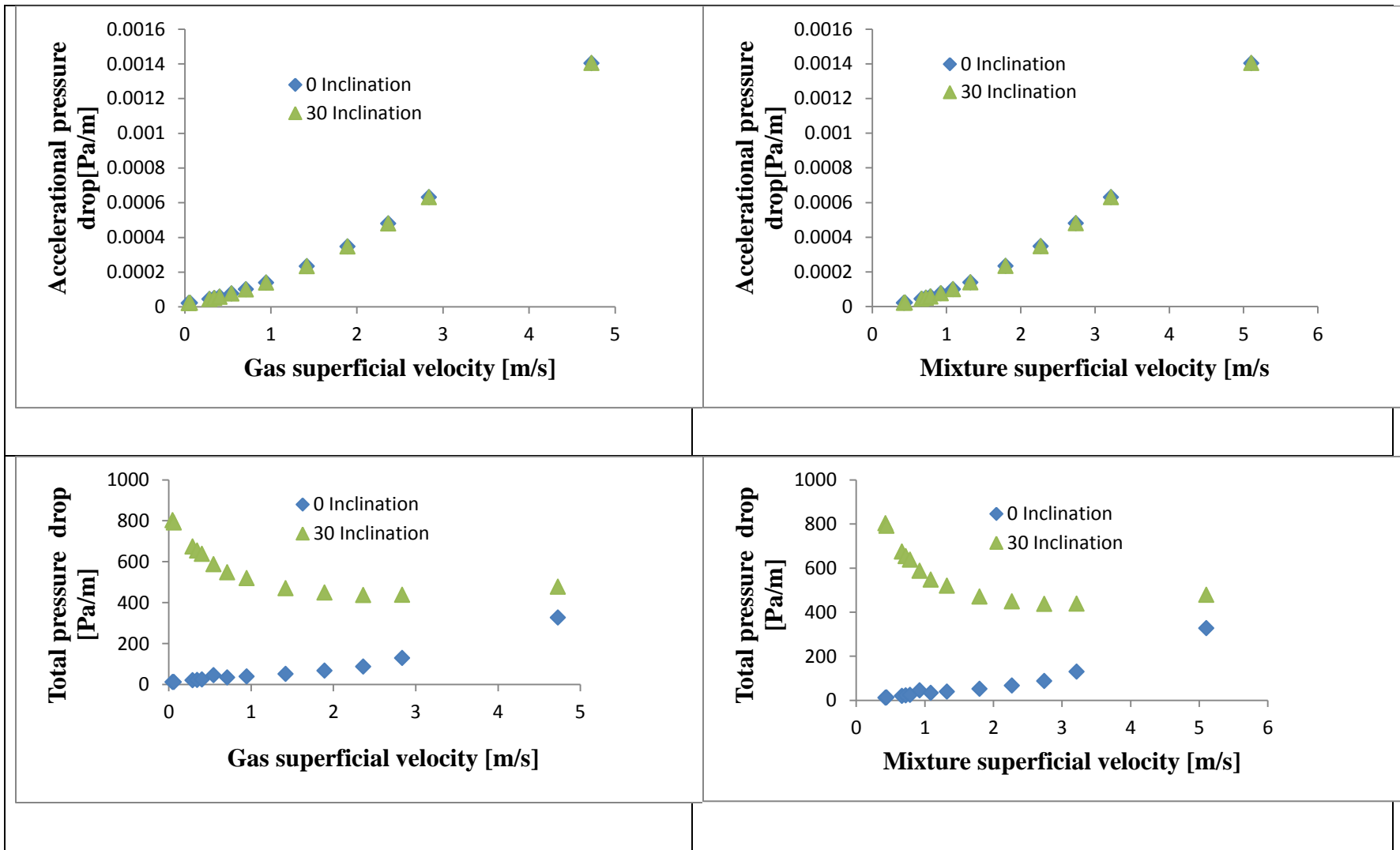


Figure 4.10 Influence of gas superficial velocities on the accelerational and total pressure gradient

Figures 4.9 and 4.10 clearly indicates that for the  $0^\circ$  inclination angle, the main contributor to the total pressure gradient is the frictional shear stress and acceleration component, which is dependent on the mixture density, which in turn is a function of the in-situ volume fraction or liquid holdup. However, there is an increase in total pressure gradient when the inclination angle increases from  $0^\circ$  to  $30^\circ$  as depicted from the above Figure 4.9 and 4.10.

It is interesting to note that for a given liquid superficial velocity, there is no great effect in both the frictional and acceleration pressure gradient as gas superficial velocity increases in the two inclination angles considered. However, in the case of the gravitational component there exist increase in pressure gradient as both gas and mixture superficial velocities increases. This contributes to the overall total pressure gradient predicted in the angles considered in this experiment. Mattar and Gregory (1974), Spedding and Chen (1981), Barnea et al (1985), Roumazelles et al. (1994) concluded in their work that larger bubbles are formed due to coalescence, which causes a decrease in the liquid velocity due to higher level of liquid holdup, hence increasing the frictional pressure gradient.

#### **4.5 Structure velocity**

A cross-correlation was performed between the time varying void fraction data measured by the twin ECT-planes positioned at 4.400 m and 4.489 m above the mixing chamber at the bottom of the riser. The evaluation of the time delay for individual slug to travel from ECT-plane-1 to ECT-plane-2 facilitated the computation of the translational velocity. A plot of structure velocity is plotted against mixture superficial velocity (where  $U_m = U_{SL} + U_{SG}$ ) as shown in Figure 4.12. A comparison between the structure velocities obtained from experiment and two major correlations is also presented here. The two correlations Bediksen (1984) and Nicklin et al. (1962) are  $UN = 1.2Um + 0.54\sqrt{gD}$  and  $UN = 1.2Um +$



$0.35\sqrt{gD}$ , respectively- Where,  $U_m$  is the mixture velocity,  $g$  is the acceleration due to gravity and  $D$  is the pipe diameter.

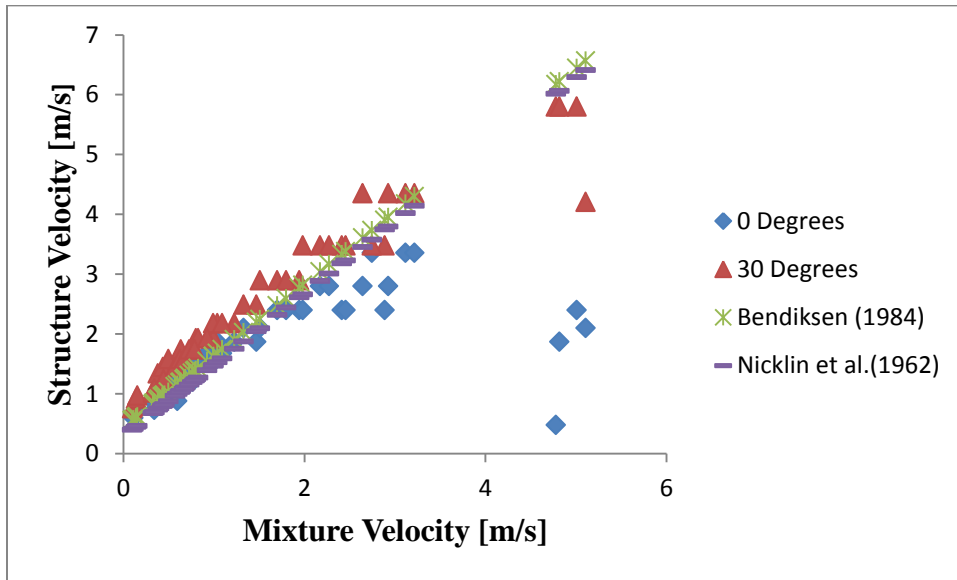


**Figure 4. 11 Structure velocity for 0° and 30° inclination angles obtained from experiments using ECT and empirical correlations of Bendiksen (1984) and Nicklin et al. (1962) correlation**

Figure 4.11 shows that both the Nicklin et al. (1962) and Bendiksen (1984) correlations predict well for both the 0° and 30° inclination angles, even though the correlation of Nicklin et al. (1962) as reported in the literature to be applicable to vertical pipes. Interestingly, in this study this correlation has been able to predict structure velocity close to the general Bendiksen correlation for predicting structure velocity-for all pipe orientations.

#### 4.6 Flow pattern map

Flow pattern map determines the transition boundaries between the different flow pattern regions as a function of the gas and liquid superficial velocities. In predicting the flow pattern map using Shoham (2006) computer codes, the fluid properties consisting of density, viscosity and surface tension were specified in the input data interface. The pipe geometry was also specified by diameter, angle and absolute roughness with the interface also specified as smooth. The calculated boundaries are then plotted in the form of a flow pattern map using  $U_{sg}$  and  $U_{sl}$  as coordinate system. The operating point will be overlaid on the general flow pattern map and the existing flow pattern can be observed on the map. Figure 4.12 (a) and (b) show the flow pattern map generated for  $0^\circ$  and  $30^\circ$  pipe inclination angle. The model adopted here was based on Taitel *et al.* (1980) for bubbly/slug transition. Moreover, slug flow was the most dominant flow pattern as observed in both inclination angles, characterized with occurrence of Taylor bubbles. The other models that could be adopted for other flow regimes are Jayanti and Hewitt (1992) or Watson and Hewitt (1999) model based on slug and churn flow transition. The flow rates at which the experiment was carried out by Abdulkadir (2011a) for liquid and gas superficial velocity were in the range of  $0.05\text{m/s} \leq U_{sl} \leq 0.38\text{m/s}$  and  $0.047\text{m/s} \leq U_{sg} \leq 4.727\text{m/s}$  respectively

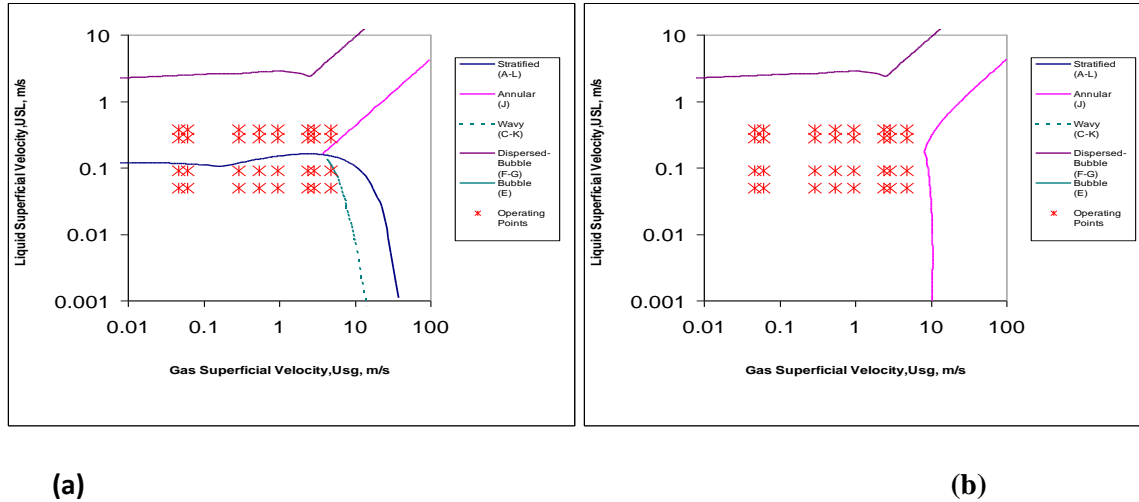
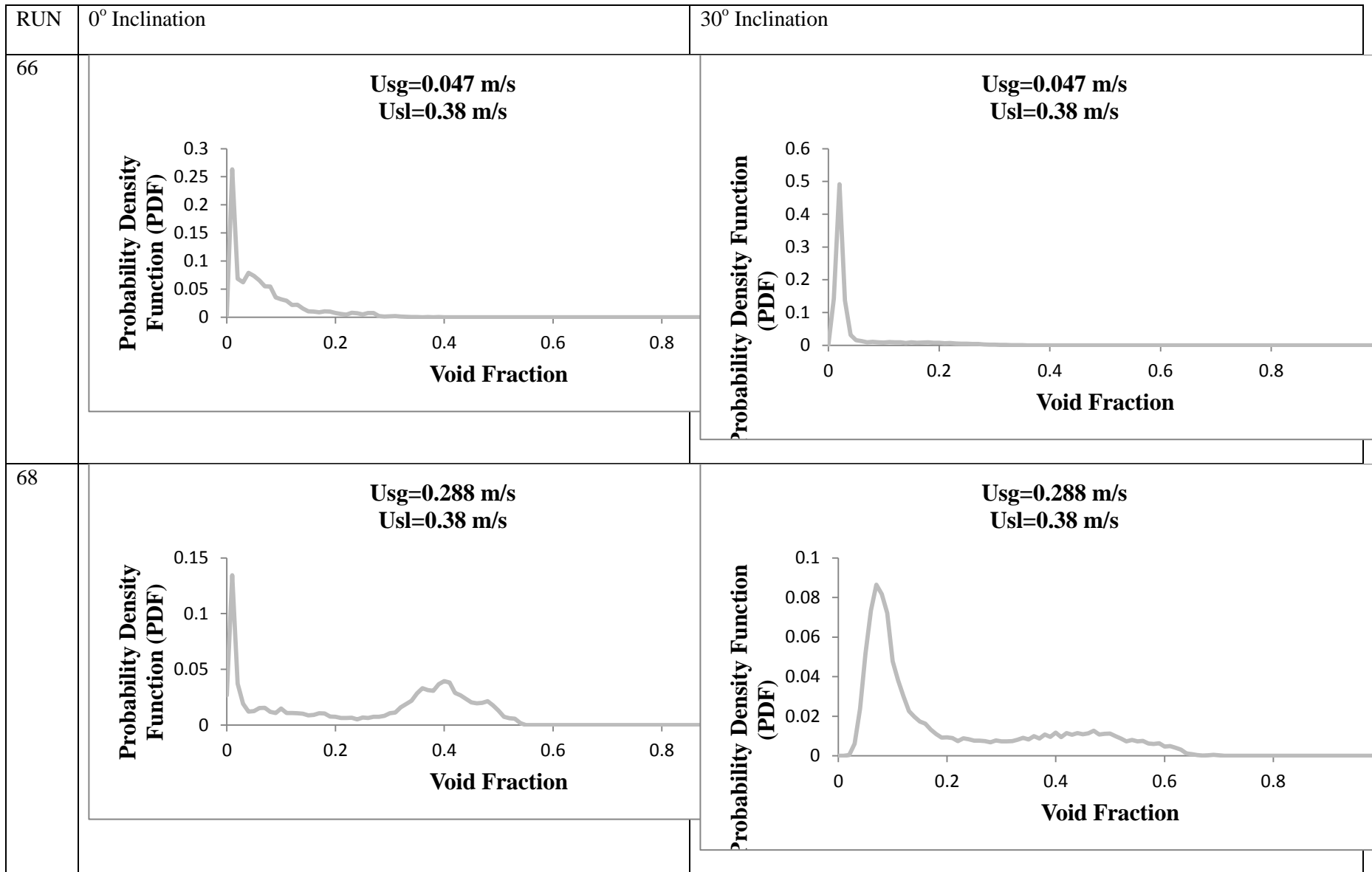


**Figure 4.12 (a) and (b)Shoham (2006) flow pattern map for 0° and 30° air/silicone mixture**

From the flow pattern map shown in figures 4.12(a) and (b) at 0° inclination most of the data points were between stratified smooth flow and slug flow regions at liquid velocity between 0.05 to 0.38- m/s. The data points that fell in the slug region can be attributed to the increase in liquid velocity from 0.28 to 0.38 -m/s. However, for the pipe inclined at 30 ° to the horizontal all the data points fell in the region of slug flow as seen in figure 4.12 (b) at the same conditions. This confirms at very small inclination angles, the force of gravity acting in the flow direction can be of the order of the wall shear stress. This interesting observation is in agreement with the conclusions made by Barnea et al (1985) in their work. This also confirms the conclusions made by Mattar and Gregory (1974) that for uphill pipe sections, slug flow was the predominant flow pattern.

#### **4.7 Probability density function (PDF)**

PDF reveals information about the frequency of occurrence of each void fraction through amplitude and time variation. Figure 4.13 shows a series of curves at different gas superficial velocities with a constant liquid superficial velocity of 0.38 m/s. Discrete random variables can be plotted in a histogram which shows the frequency (on the ordinate) as a function of some measured parameter (on the abscissa for a given class width). The frequency distribution is then a collection of classes which are of equal size and cover the entire range of data without overlapping. The PDF with a high and a low peak indicate slug flow. However, they are not clear as those of Costigan and Whalley (1997) and Omebere-Iyari and Azzopardi (2006) who worked with pipes of smaller internal diameter than the present work. Khatib and Richardson (1984) and Costigan and Whalley (1997) proposed that twin peaked probability density function (PDFs) of recorded void fractions represented slug flow. The low void fraction peak corresponds to liquid slug while the high void fraction peak is for the corresponding Taylor bubble.



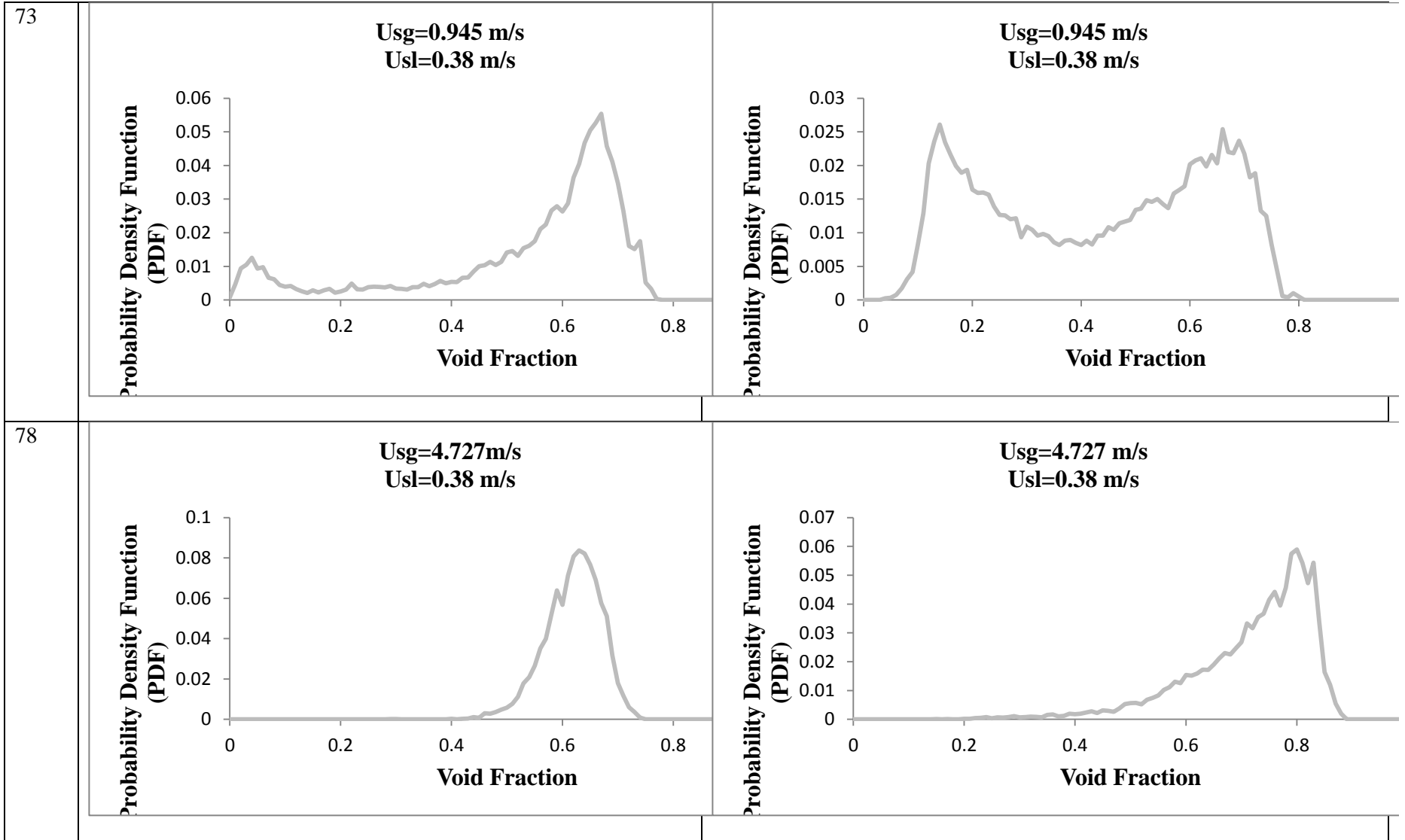


**Figure 4.13 PDF for 0° and 30° pipe inclination**

## 4.8 Frequency

Gregory and Scott (1969) developed a much used correlation for slug frequency prediction based on the data by Hubbard (1965). The methodology of power spectral density (PSD) was used to determine the dominant frequency. Details of PSD can be found in Hubbard and Duckler (1966). The outputs from the measuring instruments were analyzed and their plots were compared for various inclination considered in this work as shown in figure 4.14 for various liquid superficial velocities using ECT.

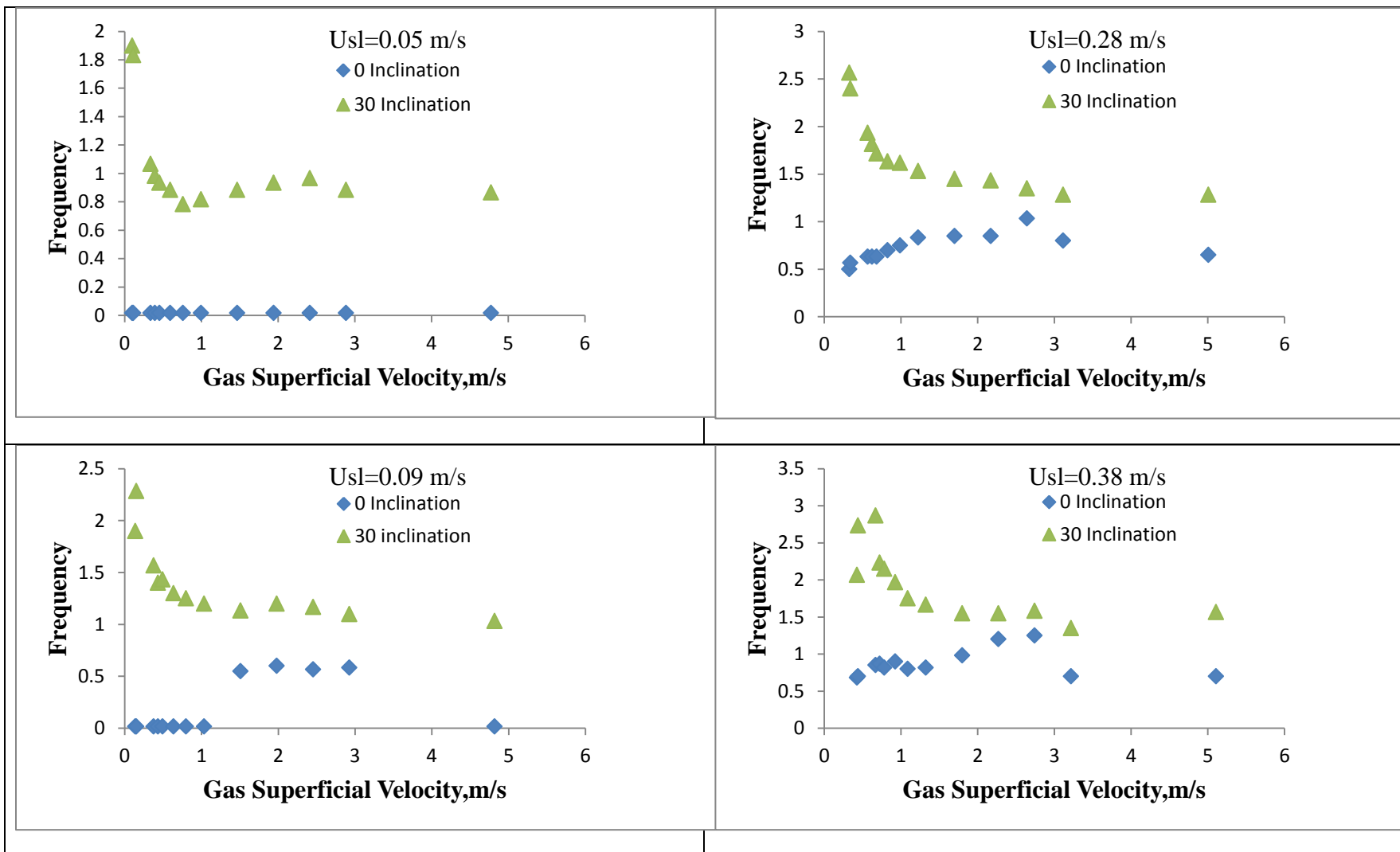


Figure 4.14 Effect of gas superficial velocity and angle of inclination on frequency for various liquid superficial velocity



Figure 4.14 shows that at constant liquid superficial velocity of 0.05-m/s and  $0^\circ$  inclination there is a constant frequency of 0.0166-Hz for the range of  $U_{sg}$  considered. However, in the case of  $30^\circ$  inclination angle there is a decrease in frequency from 1.9 - 0.86- Hz at the same constant liquid superficial velocity. Increasing the liquid superficial velocity from 0.05-0.38 m/s brings about an increase in frequency for the  $0^\circ$  and  $30^\circ$  inclination angles.

## CHAPTER 5

### CONCLUSIONS AND RECOMMENDATIONS

In this work an extensive study of effect of pipe inclination has been presented. Liquid holdup, pressure drop, structure velocity and frequency for different inclination angles and flow rates were estimated using experimental data. These data were then analyzed. The analysis was carried out by varying liquid and gas velocities and inclination. This has given a good insight into the phenomena that occur in inclined pipes. The summarized points below in this chapter give the final conclusions drawn from this study. Further work is also proposed, in order to improve and expand the knowledge of multiphase flow in inclined pipes.

#### 5.1 Conclusions

- Pipe inclination effect has been successfully investigated using ECT instrument. From the analysis made in chapter four it can be concluded- that pipe- inclination has some effects on the gas-liquid flows. The lengths of the Taylor bubbles, and the slug units were found to increase with increasing gas superficial velocity. Though, the length of the liquid slug was found to be varying due to a coalescence of the dispersed bubbles from the wake of a Taylor bubble.
- The slug frequency was found to generally decrease with increasing gas superficial velocity at lower liquid superficial velocity. However, at higher liquid superficial velocities, the slug frequency increases with increasing gas superficial velocity.
- Beggs and Brill (1973) correlation for pressure gradient prediction was used to calculate the pressure gradient in this study. The correlation predicts that as the pipe inclination increases

from  $0^\circ$  to  $30^\circ$  there is a general increase in gravitational, frictional and acceleration pressure drop, hence an increase in the overall total pressure drop.

- In this work none of the void fraction correlation predicted perfectly for both the  $0^\circ$  and  $30^\circ$  pipe inclination. However, Guzhov et al. (1967) and Flanigan (1958) are the best performing correlation based on the drift flux model for both inclination.
- A linear relationship was obtained between structure velocity and mixture superficial velocity. A comparison of this data with the empirical relationships proposed the Nicklin et al. (1962) and Bendiksen (1984) correlations predict well for both the  $0^\circ$  and  $30^\circ$  inclination angles. Even though the correlation of Nicklin et al. (1962) as reported in the literature to be applicable to vertical pipes.

## **5.2 Recommendations**

- A similar comparative analysis should be carried out on the effect of pipe inclination on void fraction distributions for inclinations higher than  $30^\circ$ .
- Investigating the effect of fluid properties (density, viscosity, and surface tension) would be of particular interest in the oil and gas industry applications where liquids and gases have different properties.
- Finally, computational fluid dynamics should be employed to validate the void fraction distribution in pipe inclination.

## NOMENCLATURE

Symbol	Description	Units
A	Cross-sectional Area	$m^2$
$C_o$	Distribution parameter	Dimensionless
D	Diameter of pipe	m
$H_L$	Liquid-holdup	Dimensionless
$F_r$	Froude number, $\frac{U_M^2}{gD}$	Dimensionless
f	Frequency	$H_z$
g	Acceleration of gravity	$ms^{-2}$
G	Mass flux	$Kgm^{-2}S$
L	Length	m
m	Mass	$K_g$
$\rho$	Density	$Kgm^{-3}$
$Re_M$	Mixture Reynolds number	Dimensionless
S	Slip ratio	Dimensionless
$\mu$	Viscosity	$Kgm^{-1}S^{-1}$
$U_g$	Velocity of gas	$ms^{-1}$
$U_{GM}$	Drift velocity, $U_G - U_M$	$ms^{-1}$
$U_L$	Velocity of liquid	$ms^{-1}$
$U_M$	Mixture velocity, $U_{SL} - U_{SG}$	$ms^{-1}$
$U_{SG}$	Superficial gas velocity	$ms^{-1}$
$U_{SL}$	Superficial Liquid velocity	$ms^{-1}$

X	quality, mass of Vapour /total mass	Dimensionless
T	Temperature	°C
P	Pressure	$Nm^{-2}$

### Greek Letters

$\varepsilon$	Void fraction, average
$U_{SL}$	No slip (homogeneous) void fraction
$\beta$	Volumetric quality, $\varepsilon_H$
$\lambda$	Input liquid content, $\frac{U_{SL}}{U_{SL}+U_{SG}}$
$\mu$	Viscosity
$\rho$	Density
$\theta$	Pipe inclination angle

### Subscripts

G	Gas Phase
L	Liquid Phase
M	Mixture
S	Superficial

## APPENDICES

### APPENDIX A

### DATA TEST MATRIX FOR 67mm 0° PIPE INCLINATION

<b>RUN</b>	<b>Usl[m/s]</b>	<b>Usg[m/s]</b>	<b>Um[m/s]</b>	<b>HL</b>	$\epsilon$	<b>Freq[Hz]</b>	$\delta$ [mm]	<b>Structural velocity</b>	<b>Bendiksen</b>	<b>Nicklin</b>
1	0.05	0.047	0.097	0.6274	0.3726	0.01667	13.0513	-0.084	0.55419	0.40015
2	0.05	0.061	0.111	0.6324	0.3676	0.01667	13.1889	0.6	0.57099	0.41695
3	0.05	0.288	0.338	0.5387	0.4613	0.01667	10.7471	0.73	0.84339	0.68935
4	0.05	0.344	0.394	0.5155	0.4845	0.01667	10.182	0.8	0.91059	0.75655
5	0.05	0.404	0.454	0.4834	0.5166	0.01667	9.42191	0.88	0.98259	0.82855
6	0.05	0.544	0.594	0.4111	0.5889	0.01667	7.79216	0.88	1.15059	0.99655
7	0.05	0.709	0.759	0.3731	0.6269	0.01667	6.9757	1.2	1.34859	1.19455
8	0.05	0.945	0.995	0.3312	0.6688	0.01667	6.10364	1.53	1.63179	1.47775
9	0.05	1.418	1.468	0.2384	0.7616	0.01667	4.26465	1.87	2.19939	2.04535
10	0.05	1.891	1.941	0.223	0.777	0.01667	3.97055	2.4	2.76699	2.61295
11	0.05	2.363	2.413	0.1698	0.8302	0.01667	2.97637	2.4	3.33339	3.17935
12	0.05	2.836	2.886	0.2196	0.7804	0.01667	3.90602	2.4	3.90099	3.74695
13	0.05	4.727	4.777	0.2652	0.7348	0.01667	4.78364	0.48	6.17019	6.01615

27	0.09	0.047	0.137	0.9144	0.0856	0.01667	23.6987	0.73	0.60219	0.44815
28	0.09	0.061	0.151	0.8996	0.1004	0.01667	22.8852	0.76	0.61899	0.46495
29	0.09	0.288	0.378	0.7049	0.2951	0.01667	15.3018	1.05	0.89139	0.73735
30	0.09	0.344	0.434	0.6594	0.3406	0.01667	13.9491	1.12	0.95859	0.80455
31	0.09	0.404	0.494	0.6254	0.3746	0.01667	12.9965	1.2	1.03059	0.87655
32	0.09	0.544	0.634	0.531	0.469	0.01667	10.558	1.4	1.19859	1.04455
33	0.09	0.709	0.799	0.4774	0.5226	0.01667	9.28249	1.53	1.39659	1.24255
34	0.09	0.945	1.035	0.4277	0.5723	0.01667	8.15708	1.87	1.67979	1.52575
35	0.09	1.418	1.508	0.2963	0.7037	0.55	5.39791	2.1	2.24739	2.09335
36	0.09	1.891	1.981	0.2536	0.7464	0.6	4.55786	2.4	2.81499	2.66095
37	0.09	2.363	2.453	0.2393	0.7607	0.56667	4.28193	2.4	3.38139	3.22735
38	0.09	2.836	2.926	0.2199	0.7801	0.58333	3.9117	2.8	3.94899	3.79495
39	0.09	4.727	4.817	0.3293	0.6707	0.01667	6.06475	1.87	6.21819	6.06415
53	0.28	0.047	0.327	0.9302	0.0698	0.5	24.6494	0.88	0.83019	0.67615
54	0.28	0.061	0.341	0.9171	0.0829	0.56667	23.8546	0.93	0.84699	0.69295
55	0.28	0.288	0.568	0.7316	0.2684	0.63333	16.1445	1.2	1.11939	0.96535
56	0.28	0.344	0.624	0.6947	0.3053	0.63333	14.9899	1.29	1.18659	1.03255

57	0.28	0.404	0.684	0.6738	0.3262	0.63333	14.3668	1.29	1.25859	1.10455
58	0.28	0.544	0.824	0.5893	0.4107	0.7	12.0312	1.53	1.42659	1.27255
59	0.28	0.709	0.989	0.5341	0.4659	0.75	10.6339	1.68	1.62459	1.47055
60	0.28	0.945	1.225	0.4581	0.5419	0.83333	8.83936	1.87	1.90779	1.75375
61	0.28	1.418	1.698	0.3525	0.6475	0.85	6.54343	2.4	2.47539	2.32135
62	0.28	1.891	2.171	0.3029	0.6971	0.85	5.53001	2.8	3.04299	2.88895
63	0.28	2.363	2.643	0.2735	0.7265	1.03333	4.94629	2.8	3.60939	3.45535
64	0.28	2.836	3.116	0.2805	0.7195	0.8	5.08418	3.36	4.17699	4.02295
65	0.28	4.727	5.007	0.3725	0.6275	0.65	6.96301	2.4	6.44619	6.29215
66	0.38	0.047	0.427	0.9374	0.0626	0.68333	25.1183	0.99	0.95019	0.79615
67	0.38	0.061	0.441	0.9204	0.0796	0.7	24.0485	1.05	0.96699	0.81295
68	0.38	0.288	0.668	0.7505	0.2495	0.85	16.7668	1.4	1.23939	1.08535
69	0.38	0.344	0.724	0.7249	0.2751	0.86667	15.9293	1.4	1.30659	1.15255
70	0.38	0.404	0.784	0.6976	0.3024	0.81667	15.078	1.53	1.37859	1.22455
71	0.38	0.544	0.924	0.993	0.007	0.9	30.6972	1.68	1.54659	1.39255
72	0.38	0.709	1.089	0.5652	0.4348	0.8	11.4103	1.68	1.74459	1.59055
73	0.38	0.945	1.325	0.4696	0.5304	0.81667	9.10243	2.1	2.02779	1.87375



74	0.38	1.418	1.798	0.3673	0.6327	0.98333	6.85328	2.4	2.59539	2.44135
75	0.38	1.891	2.271	0.3192	0.6808	1.2	5.85895	2.8	3.16299	3.00895
76	0.38	2.363	2.743	0.3032	0.6968	1.25	5.53603	3.36	3.72939	3.57535
77	0.38	2.836	3.216	0.3406	0.6594	0.7	6.29684	3.36	4.29699	4.14295
78	0.38	4.727	5.107	0.3863	0.6137	0.7	7.25643	2.1	6.56619	6.41215

**APPENDIX B DATA TEST MATRIX FOR 67mm 30° PIPE INCLINATION**

<b>RUN</b>	<b>Usl[m/s]</b>	<b>Usg[m/s]</b>	<b>Um[m/s]</b>	<b>HL</b>	$\epsilon$	<b>Freq[Hz]</b>	$\delta$ [mm]	<b>Structural velocity</b>	<b>Bendiksen</b>	<b>Nicklin</b>
1	0.05	0.047	0.097	0.9259	0.0741	1.9	24.3809	0.76	0.55419	0.40015
2	0.05	0.061	0.111	0.9053	0.0947	1.83333	23.1909	0.79	0.57099	0.41695
3	0.05	0.288	0.338	0.6762	0.3238	1.06667	14.4374	1.09	0.84339	0.68935
4	0.05	0.344	0.394	0.638	0.362	0.98333	13.3442	1.16	0.91059	0.75655
5	0.05	0.404	0.454	0.6117	0.3883	0.93333	12.6249	1.24	0.98259	0.82855
6	0.05	0.544	0.594	0.5316	0.4684	0.88333	10.5727	1.58	1.15059	0.99655
7	0.05	0.709	0.759	0.4899	0.5101	0.78333	9.57387	1.74	1.34859	1.19455
8	0.05	0.945	0.995	0.4361	0.5639	0.81667	8.34375	1.93	1.63179	1.47775

9	0.05	1.418	1.468	0.3686	0.6314	0.88333	6.88067	2.49	2.19939	2.04535
10	0.05	1.891	1.941	0.3215	0.6785	0.93333	5.90568	2.9	2.76699	2.61295
11	0.05	2.363	2.413	0.2799	0.7201	0.96667	5.07233	3.48	3.33339	3.17935
12	0.05	2.836	2.886	0.2532	0.7468	0.88333	4.55011	3.48	3.90099	3.74695
13	0.05	4.727	4.777	0.182	0.818	0.86667	3.20148	5.8	6.17019	6.01615
27	0.09	0.047	0.137	0.9424	0.0576	1.9	25.46	0.92	0.60219	0.44815
28	0.09	0.061	0.151	0.925	0.075	2.28333	24.3256	0.97	0.61899	0.46495
29	0.09	0.288	0.378	0.7343	0.2657	1.56667	16.2321	1.34	0.89139	0.73735
30	0.09	0.344	0.434	0.7073	0.2927	1.4	15.3759	1.45	0.95859	0.80455
31	0.09	0.404	0.494	0.6852	0.3148	1.43333	14.7041	1.58	1.03059	0.87655
32	0.09	0.544	0.634	0.6068	0.3932	1.3	12.4936	1.74	1.19859	1.04455
33	0.09	0.709	0.799	0.5523	0.4477	1.25	11.085	1.93	1.39659	1.24255
34	0.09	0.945	1.035	0.5052	0.4948	1.2	9.93542	2.18	1.67979	1.52575
35	0.09	1.418	1.508	0.4364	0.5636	1.13333	8.35045	2.9	2.24739	2.09335
36	0.09	1.891	1.981	0.3731	0.6269	1.2	6.9757	3.48	2.81499	2.66095
37	0.09	2.363	2.453	0.3374	0.6626	1.16667	6.23092	3.48	3.38139	3.22735
38	0.09	2.836	2.926	0.3041	0.6959	1.1	5.55409	4.35	3.94899	3.79495

39	0.09	4.727	4.817	0.2232	0.7768	1.03333	3.97435	5.8	6.21819	6.06415
53	0.28	0.047	0.327	0.9577	0.0423	2.56667	26.6101	1.02	0.83019	0.67615
54	0.28	0.061	0.341	0.9412	0.0588	2.4	25.3767	1.09	0.84699	0.69295
55	0.28	0.288	0.568	0.7785	0.2215	1.93333	17.7336	1.45	1.11939	0.96535
56	0.28	0.344	0.624	0.7482	0.2518	1.81667	16.6898	1.58	1.18659	1.03255
57	0.28	0.404	0.684	0.7244	0.2756	1.71667	15.9133	1.58	1.25859	1.10455
58	0.28	0.544	0.824	0.6558	0.3442	1.63333	13.846	1.93	1.42659	1.27255
59	0.28	0.709	0.989	0.6075	0.3925	1.61667	12.5123	2.18	1.62459	1.47055
60	0.28	0.945	1.225	0.554	0.446	1.53333	11.1276	2.18	1.90779	1.75375
61	0.28	1.418	1.698	0.01418	0.98582	1.45	0.23836	2.9	2.47539	2.32135
62	0.28	1.891	2.171	0.4153	0.5847	1.43333	7.884	3.48	3.04299	2.88895
63	0.28	2.363	2.643	0.3732	0.6268	1.35	6.97781	4.35	3.60939	3.45535
64	0.28	2.836	3.116	0.3413	0.6587	1.28333	6.31129	4.35	4.17699	4.02295
65	0.28	4.727	5.007	0.2573	0.7427	1.28333	4.62969	5.8	6.44619	6.29215
66	0.38	0.047	0.427	0.9596	0.0404	2.06667	26.7666	1.16	0.95019	0.79615
67	0.38	0.061	0.441	0.9458	0.0542	2.73333	25.7009	1.24	0.96699	0.81295
68	0.38	0.288	0.668	0.7931	0.2069	2.86667	18.2621	1.58	1.23939	1.08535

69	0.38	0.344	0.724	0.7658	0.2342	2.23333	17.2879	1.74	1.30659	1.15255
70	0.38	0.404	0.784	0.7429	0.2571	2.15	16.5138	1.74	1.37859	1.22455
71	0.38	0.544	0.924	0.6754	0.3246	1.96667	14.4138	1.93	1.54659	1.39255
72	0.38	0.709	1.089	0.6193	0.3807	1.75	12.8302	2.18	1.74459	1.59055
73	0.38	0.945	1.325	0.572	0.428	1.66667	11.5837	2.49	2.02779	1.87375
74	0.38	1.418	1.798	0.4875	0.5125	1.55	9.51765	2.9	2.59539	2.44135
75	0.38	1.891	2.271	0.4343	0.5657	1.55	8.30363	3.48	3.16299	3.00895
76	0.38	2.363	2.743	0.3923	0.6077	1.58333	7.38504	3.48	3.72939	3.57535
77	0.38	2.836	3.216	0.3632	0.6368	1.35	6.76708	4.35	4.29699	4.14295
78	0.38	4.727	5.107	0.2856	0.7144	1.56667	5.18507	4.21	6.56619	6.41215

**APPENDIX C**

**BEGGS AND BRILL (1973) CORRELATION FOR**

**PRESSURE GRADIENT**

CORRELATION PREDICTION FOR 67mm 0° PIPE INCLINATION

RUN	Usl[m/s]	Usg[m/s]	Um[m/s]	HL	(dP/dz)G	(dP/dz)F	(dP/dz)Acc	(dP/dz)T
1	0.05	0.047	0.097	0.6274	0	0.84682	2.24224E-06	0.84682
2	0.05	0.061	0.111	0.6324	0	1.03836	2.72772E-06	1.03837
3	0.05	0.288	0.338	0.5387	0	4.86341	1.49925E-05	4.86343
4	0.05	0.344	0.394	0.5155	0	5.94191	1.91394E-05	5.94193
5	0.05	0.404	0.454	0.4834	0	6.99651	2.40286E-05	6.99653
6	0.05	0.544	0.594	0.4111	0	9.20246	3.71446E-05	9.20249
7	0.05	0.709	0.759	0.3731	0	12.4821	5.54953E-05	12.4822
8	0.05	0.945	0.995	0.3312	0	17.348	8.68467E-05	17.3481
9	0.05	1.418	1.468	0.2384	0	23.9823	0.000166528	23.9825
10	0.05	1.891	1.941	0.223	0	35.977	0.000266963	35.9773
11	0.05	2.363	2.413	0.1698	0	39.7768	0.000386899	39.7772
12	0.05	2.836	2.886	0.2196	0	69.6798	0.000525007	69.6804
13	0.05	4.727	4.777	0.2652	0	200.302	0.001251016	200.303
27	0.09	0.047	0.137	0.9144	0	2.04684	3.72115E-06	2.04684
28	0.09	0.061	0.151	0.8996	0	2.32985	4.30525E-06	2.32985
29	0.09	0.288	0.378	0.7049	0	7.59586	1.79056E-05	7.59587
30	0.09	0.344	0.434	0.6594	0	8.86632	2.23396E-05	8.86634
31	0.09	0.404	0.494	0.6254	0	10.3619	2.75242E-05	10.362
32	0.09	0.544	0.634	0.531	0	13.2043	4.12939E-05	13.2044

33	0.09	0.709	0.799	0.4774	0	17.3598	6.03674E-05	17.3599
34	0.09	0.945	1.035	0.4277	0	23.8864	9.26845E-05	23.8865
35	0.09	1.418	1.508	0.2963	0	31.1354	0.000174143	31.1355
36	0.09	1.891	1.981	0.2536	0	42.3092	0.000276271	42.3095
37	0.09	2.363	2.453	0.2393	0	57.4609	0.000397503	57.4613
38	0.09	2.836	2.926	0.2199	0	71.4398	0.000537538	71.4403
39	0.09	4.727	4.817	0.3293	0	251.988	0.001268735	251.989
53	0.28	0.047	0.327	0.9302	0	7.95519	1.42172E-05	7.9552
54	0.28	0.061	0.341	0.9171	0	8.38235	1.51943E-05	8.38237
55	0.28	0.288	0.568	0.7316	0	15.192	3.45071E-05	15.192
56	0.28	0.344	0.624	0.6947	0	16.8166	4.02222E-05	16.8166
57	0.28	0.404	0.684	0.6738	0	18.9549	4.67403E-05	18.955
58	0.28	0.544	0.824	0.5893	0	22.5273	6.34961E-05	22.5274
59	0.28	0.709	0.989	0.5341	0	27.6312	8.59106E-05	27.6312
60	0.28	0.945	1.225	0.4581	0	33.8803	0.000122765	33.8804
61	0.28	1.418	1.698	0.3525	0	45.2	0.000212657	45.2002
62	0.28	1.891	2.171	0.3029	0	58.9679	0.000322659	58.9683
63	0.28	2.363	2.643	0.2735	0	74.5232	0.00045139	74.5236
64	0.28	2.836	3.116	0.2805	0	101.321	0.000598463	101.321
65	0.28	4.727	5.007	0.3725	0	304.63	0.001356556	304.631
66	0.38	0.047	0.427	0.9374	0	12.2675	2.17559E-05	12.2675
67	0.38	0.061	0.441	0.9204	0	12.6863	2.29135E-05	12.6863
68	0.38	0.288	0.668	0.7505	0	20.3034	4.4958E-05	20.3034
69	0.38	0.344	0.724	0.7249	0	22.3802	5.13034E-05	22.3802



9	0.05	1.418	1.468	0.3686	304.155	36.9703	0.000166369	341.125
10	0.05	1.891	1.941	0.3215	265.433	51.728	0.000266738	317.161
11	0.05	2.363	2.413	0.2799	231.232	65.2735	0.000386369	296.506
12	0.05	2.836	2.886	0.2532	209.282	80.2475	0.000524824	289.53
13	0.05	4.727	4.777	0.182	150.747	137.911	0.001252172	288.659
27	0.09	0.047	0.137	0.9424	775.888	2.10935	3.72103E-06	777.998
28	0.09	0.061	0.151	0.925	761.583	2.39546	4.30511E-06	763.979
29	0.09	0.288	0.378	0.7343	604.805	7.91168	1.79047E-05	612.716
30	0.09	0.344	0.434	0.7073	582.607	9.50827	2.23377E-05	592.116
31	0.09	0.404	0.494	0.6852	564.438	11.3493	2.75212E-05	575.788
32	0.09	0.544	0.634	0.6068	499.984	15.0818	4.12866E-05	515.066
33	0.09	0.709	0.799	0.5523	455.178	20.0716	6.03551E-05	475.25
34	0.09	0.945	1.035	0.5052	416.456	28.194	9.26617E-05	444.651
35	0.09	1.418	1.508	0.4364	359.894	45.7579	0.000174022	405.653
36	0.09	1.891	1.981	0.3731	307.854	62.0913	0.000276057	369.946
37	0.09	2.363	2.453	0.3374	278.504	80.8251	0.000397217	359.33
38	0.09	2.836	2.926	0.3041	251.128	98.5541	0.000537147	349.682
39	0.09	4.727	4.817	0.2232	184.618	171.265	0.001269719	355.884
53	0.28	0.047	0.327	0.9577	788.467	8.18981	1.42169E-05	796.656
54	0.28	0.061	0.341	0.9412	774.902	8.6021	1.5194E-05	783.504
55	0.28	0.288	0.568	0.7785	641.142	16.163	3.4505E-05	657.305
56	0.28	0.344	0.624	0.7482	616.232	18.1077	4.02191E-05	634.34
57	0.28	0.404	0.684	0.7244	596.666	20.374	4.67367E-05	617.04
58	0.28	0.544	0.824	0.6558	540.268	25.0605	6.34883E-05	565.329



59	0.28	0.709	0.989	0.6075	500.56	31.4139	8.58972E-05	531.973
60	0.28	0.945	1.225	0.554	456.576	40.9415	0.000122734	497.518
61	0.28	1.418	1.698	0.01418	12.7782	2.06043	0.000220699	14.8389
62	0.28	1.891	2.171	0.4153	342.548	80.708	0.000322485	423.256
63	0.28	2.363	2.643	0.3732	307.936	101.496	0.000451131	409.433
64	0.28	2.836	3.116	0.3413	281.711	123.131	0.000598245	404.843
65	0.28	4.727	5.007	0.2573	212.652	210.899	0.001357428	423.552
66	0.38	0.047	0.427	0.9596	790.029	12.5574	2.17555E-05	802.586
67	0.38	0.061	0.441	0.9458	778.683	13.0355	2.2913E-05	791.719
68	0.38	0.288	0.668	0.7931	653.145	21.4526	4.49556E-05	674.598
69	0.38	0.344	0.724	0.7658	630.701	23.6392	5.13007E-05	654.341
70	0.38	0.404	0.784	0.7429	611.875	26.143	5.84799E-05	638.018
71	0.38	0.544	0.924	0.6754	556.382	31.1892	7.67264E-05	587.571
72	0.38	0.709	1.089	0.6193	510.261	37.5879	0.000100825	547.849
73	0.38	0.945	1.325	0.572	471.374	48.2043	0.00013997	519.579
74	0.38	1.418	1.798	0.4875	401.905	68.7545	0.000234148	470.66
75	0.38	1.891	2.271	0.4343	358.168	91.1058	0.000348155	449.274
76	0.38	2.363	2.743	0.3923	323.639	113.66	0.000480687	437.3
77	0.38	2.836	3.216	0.3632	299.715	138.291	0.000631536	438.007
78	0.38	4.727	5.107	0.2856	235.919	242.095	0.001404549	478.015

## REFERENCES

1. Abbas, H.A.M., 2010. "Multiphase flow rate measurement using a novel conductance venture meter": Experimental and theoretical study in different flow regimes. PhD thesis, University of Huddersfield.
2. Abdulkadir, M. "Wire Mesh Sensor Experimental Data on Vertical Pipe," University of Nottingham, School of Chemical and Environmental Engineering, UK (2011a)
3. Abdulkadir, M. "Experimental and Computational Fluid Dynamics (CFD) Studies of Gas-Liquid Flow in Bends," PhD thesis, University of Nottingham, School of Chemical and Environmental Engineering, UK (2011b), 1-384.
4. Angeli, P., Hewitt, G.F. "Drop Size Distributions in Horizontal Oil–Water Dispersed Flows," *Chem. Eng. Sci.* (2000) 55, 3133–3143.
5. Ansari, A.M. et al. "Comprehensive Mechanistic Model for Two-Phase Flow in Wellbores." *SPEPF* (May 1994) 143: *Trans., AIME*, 297.
6. Arvoha B. K., Hoffmann R., Valle A. and Halstensena M., (2012) "Estimation of volume fraction and flow regime identification in inclined pipes based on gamma measurements and multivariate calibration", *Journal Chemometrics*; Vol.26, PP. 425–434.
7. Aydelott, J.C. and Devol, W., (1987) "Cryogenic Fluid Management Technology Workshop ", NASA Conference Publication, NASA Lewis Research Centre.
8. Azzopardi, B.J (1997), "Drops in Annular Two-Phase Flow," *International Journal of Multiphase Flow* 23, 1-53
9. Bagci, S. and Al-Shareef, A. (2003), "Characterisation of slug flow in horizontal and inclined pipes". *SPE* 80930, pp.1

10. Baker, A., (1954), "Simultaneous flow of oil and gas", Oil and Gas J. Vol. 53. Pp.185
11. Barnea, D., Shoham, O., Taitel, Y. and Dukler, A. E. (1985). "Gas-liquid flow in inclined tubes: flow pattern transitions for upward flow". Chemical Engineering Science, vol. 40, pp 131-136.
12. Beggs, H.D. (1972), An experimental study of two phase flow in inclined pipes, PhD Dissertation, The University of Tulsa, Tulsa, OK, Department of Petroleum Engineering.
13. Beggs, H. D. and Brill, J. P., (1973), "A Study of Two-Phase Flow in Inclined Pipes", J. Pet. Tech., pp. 607-617.
14. Bonnecaze, R.H., Erskine, W and Greskovich, E.J. (1971), Holdup and pressure drop for two phase slug flow in inclined pipes, AIChE Journal, Vol.17, pp.1109- 1113.
15. Brauner, N., and Barnea, D., (1986), "Slug/churn transition in upward gas-liquid flow". Chemical Engineering Science 41, 159-163.
16. Christopher E. Brennen (Fundamentals of multiphase flow)
17. C. Kang and W. P. Jepsen (2002)" Flow regime transitions in large diameter inclined multiphase pipelines"
18. Cook M. and Behnia M., (2000), "Pressure Drop Calculation and Modeling of Inclined Intermittent Gas-Liquid Flow", Chemical Engineering Science, Vol.55, P.P 4699-4708.
19. Colmenares, J., Ortega, P., Padrino, J., and Trallero, J.L (2001), "Slug Flow Model for the Prediction of Pressure Drop for High Viscosity Oils in a Horizontal Pipeline," SPE 114711111.
20. Collier, J.G., and Thome, J.R., (1994), "Convective boiling and condensation". Third edition, Oxford University Press, New York pp, 134-168.

21. Costigan, G., and Whalley, P. B., (1997), "Slug flow regime identification from dynamic void fraction measurements in vertical air-water flows". *International Journal of Multiphase Flow* 23, 263-282.
22. Creutz, M., Mewes, D. (1998), "A Novel Centrifugal Gas-Liquid Separator for Catching Intermittent Flow," *Int. J. Multiphase Flow* 24, 1057-1078.
23. Da Silva, M.J., Schleicher, E., Hampel, U. (2007), "Capacitance Wire-Mesh Sensor for Fast Measurement of Phase Fraction Distributions," *Measurement Science and Technology* 18, 2245-2251
24. Da Silva, M.J., Thiele, S., Abdulkareem, L., Azzopardi, B.J., Hampel, U. (2010), "High-Resolution Gas-Oil Two-Phase Flow Visualisation with a Capacitance Wire-Mesh Sensor," *Flow Measurement and Instrumentation*
25. Davies, R.M. and Taylor, G.I, (1950), "The mechanics of large bubbles rising through extended liquid and through liquids in tubes". *Proc. Roy. Soc. London*, 200A, pp.380.
26. Delhaye, J.M., Giot, M., and Riethmuller, M.L., (1981), "Thermal-hydraulics of two-phase systems for industrial design and nuclear engineering". Hemisphere McGraw-Hill Press, New York.
27. Dukler, A.E., and Taitel, Y., (1986), "Flow pattern transitions in gas-liquid systems, measurement and modeling". *Multiphase Science and Technology* 2, 53-57.
28. Duns, H.Jr. and Ros, N.C.J. (1963), "Vertical Flow of Gas and Liquid Mixtures in Wells," *Proc., Sixth World Pet. Cong., Tokyo*.
29. Elekwachi, G. K (2008), "Comparative and sensitivity study of the effects of flow parameters on pressure drop in vertical tubing". University of Alaska Fairbanks, Alaska

30. Fernandes, R. C., Semiat, R., and Dukler, A.E., (1983), "Hydrodynamics model for gas-liquid slug flow in vertical tubes". *AIChE Journal* 29, pp 981-989.
31. Geraci, G., Azzopardi, B.J., and Van Maanen (2007), H.R.E.: "Inclination Effects on circumferential Film Distribution in Annular Gas/Liquid Flows," *AIChE Journal* 53, pp 1144-1150.
32. Griffith, P., and Wallis, G. B., (1961), "Two-phase slug flow". *Journal of Heat Transfer* 83, pp 307-320.
33. Gregory, G.A. and Scott, D.S, (1969), "Correlation of liquid slug velocity and frequency in horizontal co-current gas-liquid slug flow". *AIChE Journal*, vol. 15, pp 833-835
34. Gould, T. L., Tek, M. R., and Katz, D. L., (1974), "Two-phase flow through vertical, inclined or curved pipes", *J. Pet. Tech.*, Vol. 19, PP. 815-828.
35. Gokcal, B. (2005), "Effects of High Oil Viscosity on Two-Phase Oil-Gas Flow Behavior in Horizontal Pipes," M.S. Thesis, University of Tulsa.
36. Gokcal, B. (2008), "An Experimental and Theoretical Investigation of Slug Flow for High Oil Viscosity in Horizontal Pipes," Ph.D. Dissertation, University of Tulsa.
37. Gopal M., (1994), "Visualization and Mathematical Modeling of Horizontal Multiphase Slug Flow", Ph.D. Thesis, University of Nottingham.
38. Govier, G.W., and Aziz, K., (1972), "Flow of complex mixtures in pipes". Princeton, New Jersey, USA: Van-Nostrand-Reinhold.
39. Hernandez-Perez, V., (2008), "Gas-liquid two-phase flow in inclined pipes". PhD thesis, University of Nottingham.

40. Hernandez-Perez, V. and Azzopardi, B. J. (2006), "Effect of Inclination on Gas-Liquid Flows," 10th Int. Conf., Multiphase Flow in Industrial Plant, Tropea, Italy.
41. Hernandez-Perez, V. (2007), "Gas-Liquid Two-Phase Flow in Inclined Pipes," PhD Thesis, University of Nottingham, School of Chemical, Environmental and Mining Engineering, UK, pp 1-294.
42. Hernandez Perez, V., Azzopardi, B.J., Morvan, H. (2007), "Slug flow in Inclined Pipes," In: Proceedings of 6th International Conference on Multiphase Flow 2007, Leipzig, Germany.
43. Hewitt G. F., (1978), "Measurements of two-phase flow parameters". London: Academic Press.
44. Hewitt G. F., (1982), "Flow regimes". Handbook of multiphase systems, ed. Hetsroni. Hemisphere Publication Corporation, New York.
45. Hubbard, M.G., (1965), "An analysis of horizontal gas liquid slug". PhD Thesis, University of Houston, USA
46. Hubbard, M. B., and Dukler, A.E., (1966), "The characterisation of flow regimes for horizontal two-phase flow". Proceedings of 1966 Heat Transfer and Fluid Mechanics Institution pp 101-121.
47. James P. Brill and Hemanta Mukherjee (1999), "Multiphase Flow in Wells",pp.19.
48. J. Nucl. Sci. Technology. (2003) pp 40, 932–940.
49. Jayanti, S., and Hewitt, G.F., (1992), "Prediction of the slug-to-churn flow transition in vertical two-phase flow". International Journal of Multiphase Flow pp 18, 847-860.

50. Jayanti, S., Hewitt, G.F. & White, S.P., (1990), "Time-dependent behavior of the liquid film in horizontal annular flow". *Int. Journal of Multiphase Flow*. Vol. 16.
51. Jones, O.C., and Zuber, N., (1975), "The interrelation between void fraction fluctuations and flow pattern in two-phase flow". *International Journal of Multiphase flow* pp 273.
52. Kang, C., Wilkens, R. and Jepson, W. P., (1996), "The Effect of Slug Frequency on Corrosion in High Pressure, Inclined Pipelines," NAICE 96, Paper No. 20, Denver, CO.
53. Keska, J.K., and Williams, B.E., (1999), "Experimental comparison of flow pattern detection techniques for air-water mixture flow". *Experimental Thermal Fluid Science* 19, pp 1-12.
54. Kendoush, A.A., and Sarkis, Z.A (2002), "Void Fraction Measurement by X-ray Absorption," *Exp. Therm. Fluid Sci.* 25, 615–621
55. Kokal, S.L., Stanislav, J.F., (1989). "An experimental study of two-phase flow in slightly inclined pipes- 1. Flow patterns". *Chemical Engineering Science*, Vol. 44, No 3, pp 665-679.
56. .Kokal, S. (1987), "An Experimental Study of Two Phase Flow in Inclined Pipes". PhD Dissertation, University of Calgary.
57. Kristiansen, O., (2004), "Experiments on the transition from stratified to slug flow in multiphase pipe flow". Ph.D. Thesis, NTNU, Trondheim, Norway.
58. Kutataledze, S.S., Nakoryakov, V.E., Burdukov, A.P., Tatevpsyan, Y.V., and Kuzmin, V.A., (1972), "Spectral characteristics of vertical two-phase flow". *Sov. Phys. Dokl.* 16, 718-719.

59. Kumar, S.B., Moslemian, D. and Dudukovi, M.P. (1995), “An X-ray Tomographic Scanner for Imaging Voidage Distribution in Two-Phase Flow Systems,” *Flow Measur. Instrum.* 6, 61–73
60. Legius, H. J. W. M., (1997), “Propagation of pulsations and waves in two-phase pipe systems”. PhD thesis, Delft University of Technology, Netherlands.
61. Lewis S., Fu W.L., Kojasoy G., (2002), "Internal Flow Structure Description Of Slug Flow-Pattern In A Horizontal Pipe', *International Journal of Heat and Mass Transfer*, Vol.45, P.P.3897–3910,.
62. Mattar, L. and Gregory, G.A. (1974), “Air oil slug flow in an upward-inclined pipe-I: Slug velocity, holdup and pressure gradient”, *Journal of Canadian Petroleum Technology*, Vol. 13, no.1, pp.69-76.
63. Matsui, G., (1984), “Identification of flow regimes in vertical gas-liquid two-phase flow using differential pressure fluctuations”. *International Journal of Multiphase flow* 10, 711-719.
64. Mao, Z. S., and Dukler, A.E., (1993), “The myth of churn flow”. *International Journal of Multiphase flow* 19, 377-383.
65. McQuillan, K.W., and Whalley, P.B., (1985), “Flow patterns in vertical two-phase flow”. *International Journal of Multiphase Flow* 11, 161-175.
66. Mishima, K., and Ishii, M., (1984), “Flow regime transition criteria for upward two-phase flow in vertical tubes”. *International Journal of Heat & Mass Transfer* 27, 723-737.
67. Ombebere-Iyari, N. K., (2006), “The Effect of Pipe Diameter and Pressure in Vertical Two Phase Flow”, PhD thesis, university of Nottingham.



68. Nishikawa, K., Sekoguchi, K., and Fukano, T., (1969), "On the pulsation phenomena in gas-liquid two-phase flow". *Bulletin JSME* 12, 1410-1416.
69. Ovadia Shoham, (2006), "Mechanistic Modelling of Gas-Liquid Two-Phase Flow in Pipes". pp.1.
70. P. Abduvayt (2003), "Effects of pressure and flow rate on gas-liquid two-phase flow behavior in pipelines".
71. Pietruske, H., Prasser, H. M. (2007), "Wire-mesh Sensors for High-Resolving Two-Phase Flow Studies at High Pressures and Temperatures," *Flow Measurement and Instrumentation* 18, pp 87–94.
72. Prasser, H. M., Bottger, A., and Zschau, J. (1998), "A New Electrode-Mesh Tomograph for Gas Liquid Flows," *Flow Measurement and Instrumentation* 9, pp 111-119.
73. Prasser, H.M., Misawa, M., Tiseanu, I. (2005), "Comparison between Wire-Mesh Sensor and Ultra-Fast X-ray Tomograph for an Air–Water Flow in a Vertical Pipe," *Flow Measurement and Instrumentation* 16, pp 73–83.
74. Ribeiro M., Ferreira V., Campos L.M., (200), "On The Comparison Of New Pressure Drop And Hold-Up Data For Horizontal Air–Water Flow In A Square Cross Section Channel Against Existing Correlations And Models", *International Journal of Multiphase Flow*, Vol.32, P.P. 1029–1036.
75. Richter, S., Aritomi, M., Prasser, H.M., and Hampel, R. (2002), "Approach toward Spatial Phase Reconstruction in Transient Bubbly Flow Using a Wire Mesh Sensor," *Int. J. Heat Mass Transfer* 45, 1063–1075

76. Roumazeilles, P.M., Yang, J., Sarica, C., Chen, X., Wilson, J., and Brill, J.P. (1994), "An Experimental Study on Downward Slug Flow in Inclined Pipes" Annual Technical Conference and Exhibition held in New Orleans, LA., U.S.A., PP.25-28.
77. S. KOKAL and J.F. STANISLAV (1986), "An analysis of two-phase flow in inclined pipes with zero net liquid production"
78. Scott, S.L. and Kouba, G.E., (1990), "Advances in Slug Flow Characterization for Horizontal and Slightly Inclined Pipelines". SPE 20628, SPE Annual Technical Conference and Exhibition, New Orleans.
79. Sevigny, Rene: (1962), "An Investigation of Isothermal, Coeurrent, Two-Fluid Two-Phase Flow in an Inclined Tube," PhD dissertation, U. of Rochester, Rochester, N. Y.
80. Shemer, L., Barnea, D., and Roitberg, E. (2006), "Measurements of Cross-Sectional Instantaneous Phase Distribution in Gas-Liquid Pipe Flow," Department of Fluid Mechanics and Heat Transfer, Faculty of Engineering, Tel Aviv University, Tel Aviv 69978, Israel 1-8
81. Singh G. and Griffith, P. (1970), "Determination of the pressure drop optimum pipe size for a two-phase slug flow in an inclined pipe". Transactions of the ASME Series B, Journal of Engineering for Industry, 92,717-726
82. Spedding, P. L. and Nguyen, V. T., (1976), "Regime maps for air-water two-phase flow", Chemical Engineering Science, Vol. 35, PP. 779-793.
83. Taitel, Y., Barnea, D. and Dukler, A. E. (1980) "Modelling flow pattern transitions for steady upward gas-liquid flow in vertical tubes". The AIChE Journal, Volume 26(3), pp. 345-354.

84. Taitel, Y., (1986), "Stability of severe slugging". *International Journal of Multiphase flow* 12, 203-217.
85. Taitel, Y., (2000), "Two-phase gas-liquid flow short course - Fundamentals of multiphase flow modelling". Department of Fluid Mechanics and Heat Transfer, Tel Aviv University.
86. Taitel, Y, and Dukler A.E., (1976), "A model for predicting flow regime transitions in horizontal and near horizontal gas - liquid flow". *AICRE Journal*. Vol. 22, NO.1, pp. 52.
87. Thome, J.R.: "Engineering Data Book III," Laboratory of Heat and Mass Transfer (LTCM), Faculty of Engineering Science and Technology, Swiss Federal Institute of Technology Lausanne (EPFL), Wolverine Tube, Inc., CH-1015 Lausanne, Switzerland
88. Tutu, N.K., (1982), "Pressure fluctuations and flow pattern recognition in vertical two-phase gas-liquid flows". *International Journal of Multiphase flow* 8, 443.
89. Ullmann A., Zamir M., Ludmer Z., Brauner N., (2003)," Stratified Laminar Countercurrent Flow Of Two Liquid Phases In Inclined Tubes", *International Journal of Multiphase Flow* (29) p.p.1583–1604,.
90. Vince, M. A., and Lahey, R. T., (1982), "On the development of an objective flow regime indicator". *International Journal of Multiphase flow*, 8, 93-124.
91. Wangjiraniran, W., Motegi, Y., Richter, S., Kikura, H., Aritomi, M., Yamamoto, K.: "Intrusive Effect of Wire Mesh Tomography on Gas-Liquid Flow Measurement,"
92. Weisman, J. and Kang, S. Y. (1981), "Flow pattern transitions in vertical and upwardly inclined lines", *International Journal of Multiphase Flow*, Volume 7(3), pp 271-291.

93. Wongwises S. and Pipathattakul M., (2006), "Flow Pattern, Pressure Drop And Void Fraction Of Two-Phase Gas-Liquid Flow In An Inclined Narrow Annular Channel", *Experimental Thermal and Fluid Science* Vol. 30, P.P. 345–354.
94. Xiao, J.J., Shoham, O., and Brill, J.P.( 1990), "A Comprehensive Mechanistic Model for Two phase Model," SPE 20631, Presented at SPE Annual Fall Meeting, New Orleans, LA, September 23-26.
95. Zoetewij, M.L., (2007), "Long liquid slugs in horizontal tubes: development study and characterization with electrical conductance techniques". PhD thesis, Delft University of Technology, Netherlands.
96. Zhang, H.-Q., Wang, Q., Sarica, C., and Brill, J.P. (2003), "Unified Model for Gas-Liquid PipeFlow via Slug Dynamics - Part 2: Model Validation," *ASME, J. Energy Res. Tech.*, Vol. 125.
97. Zheng, G. H. and Brill, J.P., Shoham, O., (1992), "An Experimental Study of Two-Phase Slug Flow in Hilly Terrain Pipelines". SPE 24788, presented in the SPE 67th Annual Technical Conference and Exhibition, Washington, DC.pp. 233
98. Zukoski, E.E. (1966), "Influence of Viscosity, Surface Tension and Inclination Angle on Motion of Long Bubbles in Closed Tubes," *J. Fluid Mech.* 25,821-37